CFD SIMULATION OF SHELL AND TUBE TYPE HEAT EXCHANGER: EFFECT OF FLOW CONDITION

WILFRED TANG KAH JUNG

This report is submitted
in fulfillment of the requirement for the degree of
Bachelor of Mechanical Engineering (Thermal-Fluid)

Faculty of Mechanical Engineering

UNIVERSITI TEKNIKAL MALAYSIA MELAKA

2017

DECLARATION

I declare that this project report entitled “CFD Simulation of Shell and Tube Type Heat Exchanger: The Effect of Flow Condition” is the result of my own work except as cited in the references.

Signature : ....

Name : ....

Date : ....

APPROVAL

I hereby declare that I have read this project report and in my opinion this report is sufficient in terms of scope and quality for the award of the degree of Bachelor of Mechanical Engineering (Thermal-Fluid).

Signature :. ....

Name of Supervisor : ....

Date : ....

DEDICATION

To my beloved mother and father

ABSTRACT

Shell and Tube Heat Exchanger (SNTHE) is widely used in the industry for heating, cooling, condensation and boiling processes with water as the most commonly used cooling fluid. This study investigates performances of SNTHE using three different fluids; Ammonia for its higher specific heat capacity than water, Carbon Dioxide for its high thermodynamics properties and Isobutane for its green refrigerant characteristics. A functional CFD model of SNTHE is developed and temperature condition, temperature contour, velocity condition and velocity contour of three different coolants are studied. Unbaffled Shell and Tube Heat Exchanger is used to simplified the shell side fluid flow as the presence of baffle will make the shell side fluid flow more complex. The model is designed as cited in the journal by Pal (2016) and the setting was set according to his paper. Model with water was used for grid independency test and validation purpose. After validation, Ammonia, Carbon Dioxide and Isobutane were set as the working fluid. The velocity contour shows that the fluids have similar pattern where flow skewed toward the outlet and have similar penetration pattern too. However, Isobutane offer the best fluid penetration in area between the tubes followed by Ammonia and lastly Carbon Dioxide. As for the temperature distribution, due to different thermal conductivity, different results were obtained. Isobutane is the best in term of heat transfer with average outlet temperature of 340 K followed by Ammonia 350 K and lastly Carbon Dioxide which is 350K. However, Carbon Dioxide offers no significant heat transfer as it is a gas with low density and low viscosity. As a result, it is not very suitable to be used unless it is in liquid form. Hence, Isobutane is the best alternatives compared to Ammonia and Carbon Dioxide as a substitute for water as a cooling fluid.

ABSTRAK

Penukar haba cengkerang dan tiub atau ringkasnya SNTHE digunakan secara meluas dalam industri untuk pemanasan, penyejukan, pemeluwapan dan proses mendidih. Cecair penyejukan yang sering digunakan dalam industri ialah air. Untuk projek ini, tiga cecair penyejuk berbeza yang digunakan adalah Ammonia, Isobutane dan Karbon Dioksida. Ammonia dipilih oleh kerana ia mempunyai kapasiti haba yang tinggi berbanding dengan air; Karbon Dioksida untik sifat thermodinamik yang tinggi dan Isobutane untuk kesifatan cecair penyejukan yang hijau. Model CFD untuk SNTHE telah dibina dan kontur halalaju, kontur suhu, agihan halalaju dan agihan suhu telah dikaji. Model SNTHE tanpa sesekat digunakan untuk mempermudahkan aliran cecair di sebelah cengkerang sebab kehadiran sesekat akan menyebabkan pengaliran di cengkerang lebih kompleks. Model ini direka berdasarkan kajian Pal (2016) dan penetapan ditetapkan mengikut kertas kerjanya. Pada permulaan, model ini diuji dengan air untuk ujian kebergantungan terhadap grid dan pengesahan. Selepas pengesahan, model ini dikaji dengan Ammonia, Karbon Dioksida dan Isobutane. Berdasarkan keputusan kontur halaju, ketiga-tiga cecair menunjukan aliran bendalir yang serupa dimana aliran bendalir condong ke arah keluar dan mempunyai corak penembusan yang sama. Walau bagaimanapun, Isobutane mempunyai penembusan cecair yang terbaik di antara tiub diikuti oleh Ammonia dan Karbon Dioksida. Bagi pengedaran suhu, oleh kerana kekonduksian haba yang berbeza, hasil berbeza diperolehi. Isobutane adalah terbaik dari segi pemindahan haba dengan purata suhu keluar 340 K diikuti oleh Ammonia 350 K dan akhir sekali Karbon Dioksida dengan suhu 350 K. Walau bagaimanapun, Karbon Dioksida tidak menunjukkan proses pemindahan haba yang ketara kerana ia adalah gas dengan kepadatan yang rendah dan kelikatan yang rendah menyebabkan ia tidak sesuai untuk digunakan. Oleh itu, Isobutane adalah alternatif yang terbaik berbanding Ammonia dan Karbon Dioksida untuk digunakan sebagai pengganti bendalir penyejuk.

ACKNOWLEDGEMENT

First, I would like to express my gratitude to my supervisor, Dr. Fatimah Al-Zahrah Mohd Sa’at, who has guided me to successfully complete my final year project with her knowledges and ideas. I also would like to thank Dr. Ernie Binti Mat Tokit and Dr. Nazri bin Md Daud for evaluating my final year project. The ideas and suggestion given were important for me to complete this project.

Besides, I also want to thank the Faculty of Mechanical Enginnering(FKM), Universiti Teknikal Malaysia Melaka (UTeM) for allowing me to use the equipment and tools which helped me to complete this project successfully.

Finally, I would like to appreciate my family and friends support and encouragement throughout the project period.

TABLE OF CONTENTS

LIST OF TABLES

LIST OF FIGURES

LIST OF ABBEREVATIONS

SNTHE	Shell and Tube Heat Exchanger
CFD	Computational Fluid Dynamics
HE	Heat Exchanger
LMTD	Log Mean Temperature Difference
ODS	Operating Deflection Shape
AHU	Air Handling Unit
R600a	Isobutane
NH_3	Ammonia
CO_2	Carbon Dioxide

LIST OF SYMBOLS

D = inner diameter of the tube

V = average velocity of the fluid

ρ = density of the fluid

μ = dynamic viscosity

$\dot{m}$ = mass flow rate

v = kinematic viscosity

Re =Reynolds Number

D_h =Hydraulic Diameter

h =Heat Transfer Coefficient

Nu =Nusselt Number

k =Thermal Conductivity

CHAPTER 1

INTRODUCTION

1.1 BACKGROUND

Shell and Tube Heat Exchangers (SNTHE) are widely used in the industry as they have flexible designs. According to Chunnangad (2006), more than 35-40% heat exchangers are SNTHE. Usually, SNTHE are found in petrochemical and food industries. Their main purpose is to perform heating, cooling, condensation and boiling process. The main reason they are preferred in the industry is because they offer wide range of temperature change, and easy to be maintained.

Figure 1.1: Shell and Tube Heat Exchanger in food industry

Figure 1.2: Shell and Tube Heat Exchanger in petrochemical industry

According to Pal (2016), SNTHE are popular in these industries because of its high rate of heat transfer in terms of volume and weight. Not only that, SHTHE can be built easily as it built from ranges tubes sizes with the strength to withstand the fabrication stress, shipping, fields erection stress and operation. Plus, the crucial SHTHE part like gasket, tubes screw can be replaced easily as all these components are easily found in the aftermarket. This makes the SNTHE to be maintained easily and cheaply.

In the industry, SNTHE are important for its ability to handle fluid of different temperature, flow rates, thermal properties and different expansion rates of metals. When mentioning handling fluids, it demotes the involvement of two or more liquids in the heat exchange process of convection and conduction. This is similar to mixing chamber where two different types of liquids with different temperature are mixed to achieve desired temperature. The difference between mixing chamber and SNTHE is that, SNTHE do not mixed the liquids to achieved desired temperature.

According to Aslam (2012), cross flow between tube banks and shell side are important aspects as it represents the ideal process in many important industry processes like flow in filtration, biological system, fibrous media or insulation material.

1.2 PROBLEM STATEMENT

Shell and Tube Heat Exchanger have been used for a century and lots of modifications and improvements are constantly done to increase the efficiency of the heat exchange rate. According to Anas (2016), shell and tube heat exchanger have gone through lots of improvement and modifications for the past century which includes the selection of better high thermal conductivity and durability material, better baffle design are determined by the optimum angle of the baffle. However, problems still occurred regarding the Shell and Tube Heat Exchanger like heat and flow problems.

SNTHE today are equipped with baffles as the main supporter for the tubes and the baffles also provide certain behaviour of shell-side flow. However, there are some problems encountered by this device. The presence of baffle affects the shell-side flow. The subsequent flow contraction and expansion has caused flow separation at the edge of the baffle causing the pressure to drop significantly.

Besides that, there are issues of 'dead zones' at some areas near baffles. The 'dead zones' are area near baffles that are not reached by the fluid. The phenomenon could happen at certain condition of fluid flow like low fluid velocity, low mass flow rate, unstable of Reynolds number and poor shell and tube heat exchanger design. This 'dead zones' will greatly affect the heat exchange rate between the inner wall and outer wall as the dead zone are the part where the heat is not reach by fluid to carry out the heat exchange process (Wang, 2010).

1.3 SCOPE

1. To use CFD software to stimulate the flow.
2. To study the temperature distribution of three different type of coolants in Shell and Tube Heat Exchanger (SNTHE)
3. To study the flow condition of three different type of coolants in Shell and Tube Heat Exchanger (SNTHE)

Computational Fluid Dynamics (CFD) will be used to simulate the flow condition in the shell and the tube heat exchangers. Ansys, Design Modeler is used as the software to draw SNTHE model and to simulate the problem. Another scope is to study the relationship of different type of coolants and heat exchange rate. Coolants are identified in terms of chemical properties, heat properties to be used to simulate its performance towards heat transfer. The next scope of this study is to study the temperature distribution inside the Shell and Tube Heat Exchanger (SNTHE). Not only that, the flow condition such as velocity vector, velocity penetration are also further studies and identified their effect on the heat exchange process.

1.4 OBJECTIVE

1. To study a functional CFD model of Shell and Tube Heat Exchanger
2. To compare the temperature distribution of three different coolant in Shell and Tube Heat Exchanger.
3. To compare the flow condition of three different coolant in Shell and Tube Heat Exchanger.

CHAPTER 2

LITERATURE REVIEW

2.1 Heat Exchanger

According to Yong (2015), heat exchangers (HE) are devices that transfers heat between one or more fluids. Fluids are usually separated by the solid wall to prevent the fluid from mixing or contacting each other. HE is very important in the industry as it is widely used in air conditioning, chemical plants, natural-gas processing, sewage treatment, space heating, petrochemical plants, petroleum refineries and power station. One of the conventional HE examples is internal combustion engine where engine coolant flows through radiator coils. At the same time, air passes through coils and cooled the coolant and heats the air. In heat exchanger, there are four basic flow configurations, counter flow heat exchanger, parallel flow heat exchanger, mixed flow heat exchanger and hybrid heat exchanger (Yong et al., 2015).

2.1.1 Counter Flow Heat Exchanger

In counter flow heat exchanger, two fluids flow in opposite directions. This type of flow allowed the biggest temperature different between both fluids to occur. Hence it is the most efficient heat exchanger in term of heat exchange rate compared to other heat exchangers.

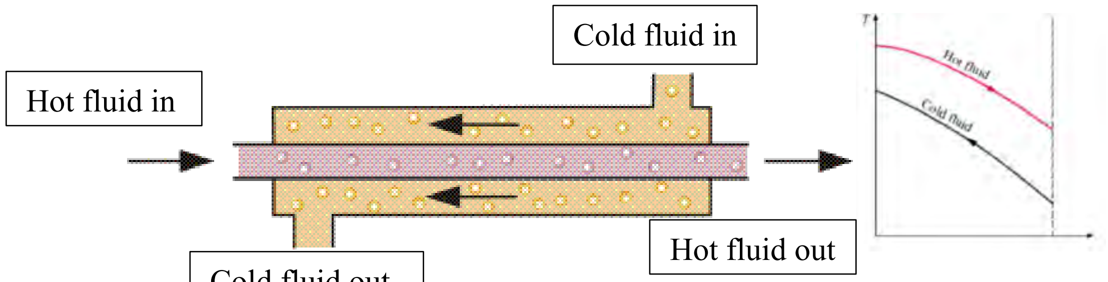

(a) (b)

Figure 2.1: (a) Counter Flow, (b) temperature profile of cross flow (Cengel and Ghajar, 2015)

According to Zhang (2016), plate heat exchanger is one of the common types of counter flow heat exchanger. Plate heat exchanger is mainly build with plates and frames. The plates are thin and large in surface area and the plates are equally separated. The gaps between the plates are usually small as small fluid flow is required to enhance the heat transfer process.

There are two types of plate heat exchangers, closed loop and open loop. For closed loop plate heat exchanger, the plates are permanently bonded by brazing and welding. Closed looped applications are like refrigeration cycle. Well for open loop plate's heat exchanger, the plates are mounted and assembled like gasket. Because of these features, it allows the plates to undergo cleaning, inspection or disassembly easily.

The plate heat exchanger will carry out heat transfer by means of conduction and convection. There are two types of plates in the plate heat exchanger. Upward flow plates and downward flow plates. These plates are arranged alternatively and the hot fluid will flow in upward flow plates while the cold will flow in downwards flow plats or vice versa (Zhang et al., 2016).

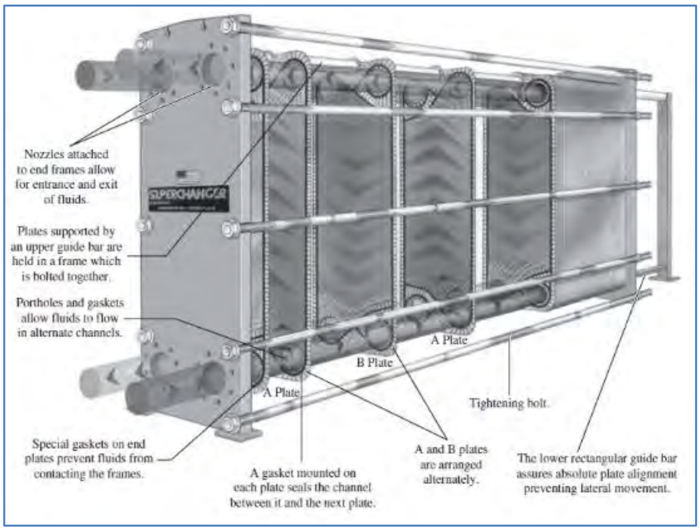

Figure 2.2: Plate Heat Exchanger (Cengel and Ghajar, 2015)

2.1.2 Parallel Flow Heat Exchanger

In parallel flow heat exchanger, the fluid flows parallelly in the same direction. Although it is less efficient than counter flow heat exchanger in terms of heat transfer, however, this kind of flow provide a more uniform wall temperature. For parallel flow type of heat exchanger, there is no specific type of heat exchanger as it can be applied for vertical and horizontal flow heat exchanger (Cengel and Ghajar, 2015).

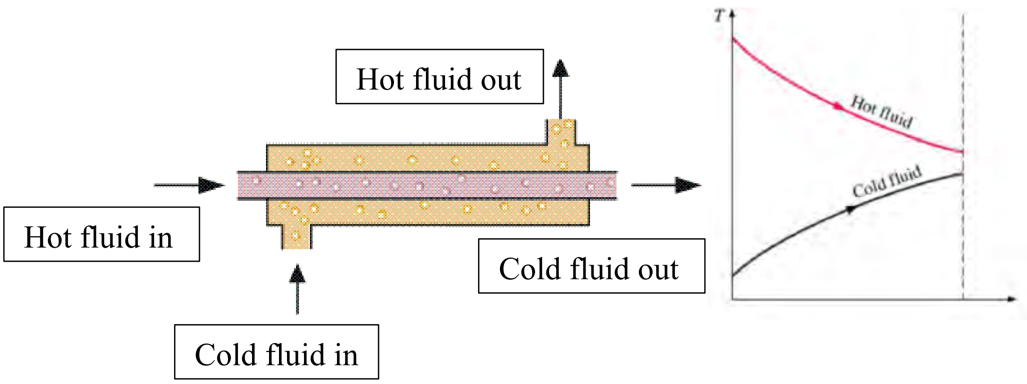

(a) (b)

Figure 2.3: (a) Parallel Flow, (b) Temperature Profile (Cengel et al., 2015)

2.1.3 Cross Flow Heat Exchanger

In cross flow heat exchanger, Brogan (2011) stated that the fluid flows at 90 degrees. For this kind flow, its efficiency is lower than counter flow but higher than parallel flows. According to Cengel and Ghajar (2015), cross flow heat exchanger can be classified as mixed and unmixed flow.

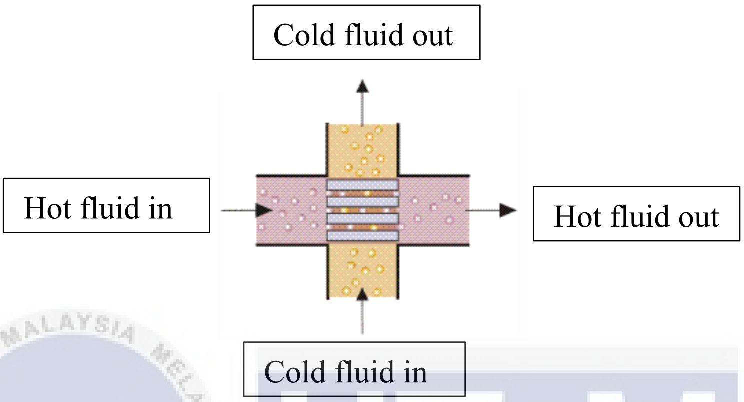

Figure 2.4: Cross Flow (Brogan, 2011)

Based on the Figure 2.5 (a), it can be observed that the flow is unmixed as the fluids are forced to flow through plate fins interfin spacing in the transverse direction. Cross-flow in (b) is categorized as mixed as the fluid is free to move in transverse direction without being confined to the plate as the model in Figure 2.5 (a).

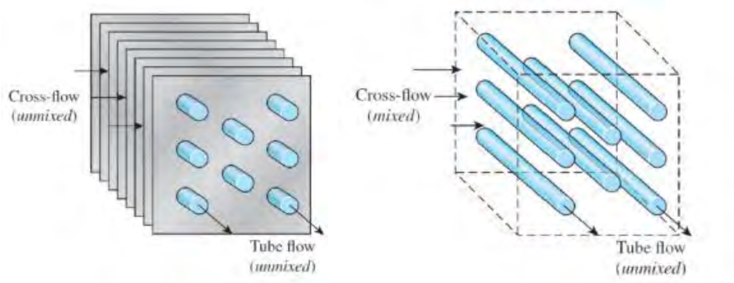

(a) Both fluids unmixed (b) one fluid unmixed, one fluid mixed

Figure 2.5: Different flow configuration in cross-flow heat exchanger (Cengel et al., 2015)

2.1.4 Hybrid Heat Exchanger

Usually in the industry, there is custom made heat exchanger which is called the hybrid heat exchanger. This kind of heat exchanger is a combination of few fluid flows such as cross flow, and counter flow.

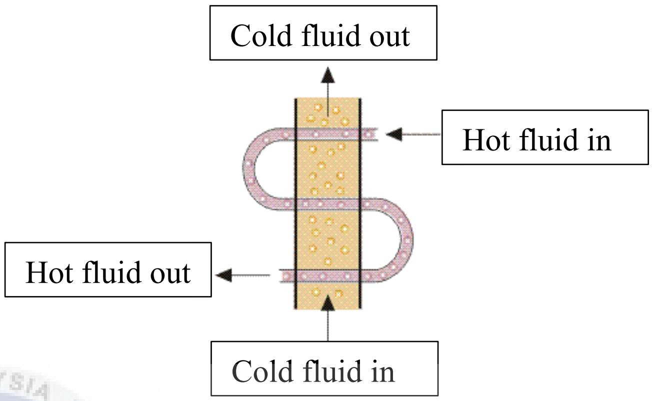

Figure 2.6: Cross Flow (Brogan, 2011)

Helical Coiled Heat Exchanger is one of heat exchangers that have hybrid fluid flow. Acc ording to Madhuri (2016), Helical Coils Heat Exchangers are often used to transfer heat in chemical reactors and agitated vessels. This is because heat transfer coefficients are higher in helical coils compared to other heat exchangers as they have more compact configuration resulting the heat transfer per unit space is greater compared to other type of heat exchanger especially straight tubes. With high heat transfer per unit space, helical coil heat exchanger is used to maintain the temperature of chemical reaction which have high heats of reaction by transferring the heat generated rapidly. With its high heat transfer per unit space, and the compact configuration of helical coils, helical coil heat exchanger can be applied in heat transfer application with space limitation like steam generation in marine.

Not only that, helical coil heat exchanger does not have radial concentration gradient as the secondary motion destroy it. Hence it is a suitable model to study the characteristic of a plug flow reactor in kinetic reactions studies. Even though without radial concentration of gradient, but the existence of self-induce radial acceleration is still available. The phenomenon is suitable for heat transfer under fluid flow without gravity such as space ship in outer space. Another application of the helical coiled tube is used to liquidified gases (Madhuri et al., 2016).

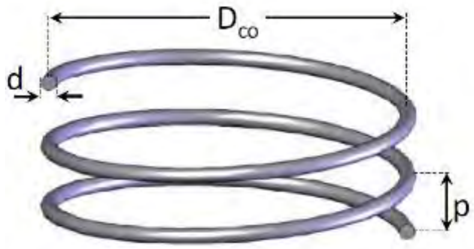

Figure 2.7: Helical coil tube (Madhuri et al., 2016)

2.2 Shell and Tube Heat Exchanger

Shell and Tube Heat Exchanger (SNTHE) is one of the most commonly used heat exchanger in industry. There are several types of SNTHE. First is SNTHE reboiler where the liquid absorbs heat from boiler to produce a gas-liquid mixture compound. Secondly, Thermosiphon Reboiler is the heat exchanger where the static head provide a natural circulation by boiling fluids. Third, is Forced Circulation Reboiler where a pump is used to move the liquid into the heat exchanger. Condenser is considered as SNTHE too as it condenses vapour by removing heat from a gas. Fifth is Chiller SNTHE which is used to cool down a medium by evaporating a refrigerant (Escoe, 1986).

SNTHE consists of tubes, shell, baffles, header and inlet, outlet valves. Hundreds of tubes bundles are usually arranged parallelly inside the shell. From tubes, heat transfer of SNTHE will occur as the one fluid flows inside the tubes while other fluids flow outside the tubes through shell. Baffles in SNTHE play key role too as it is used to maintain the uniform spacing between tubes and enhance the heat transfer of the shell-tube side fluid. Headers are used in SNTHE which it will be used to accumulate tube-side fluids before it enters and leave the tubes (Cengel and Ghajar, 2015).

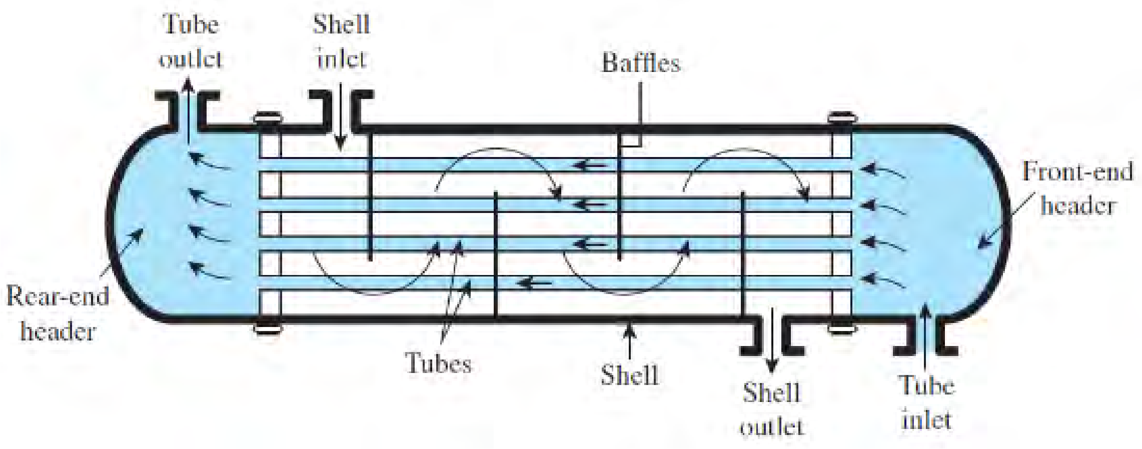

Figure 2.8: Schematic of one-shell pass and one-tube pass SNHTE (Cengel and Ghajar ,2015)

SNTHE are further classified according to the number of tubes, the type of tubes and types of shell used. According to Escoe (1986), they are several types of SNTHE. The most common one is fixed tube sheet. For this kind of heat exchanger, tube sheets are fixed to shell. Usually fixed tube sheet SNTHE is used as condenser to condense liquid to a lower temperature liquid or gas to gas or gas to liquid. Fixed tube sheet can be mounted vertically, horizontally and even used for the reboiling purposes. However, the maximum temperature it can condense is about 250^{o}F due to limitation of differential expansion of the fixed tube sheet SNTHE.

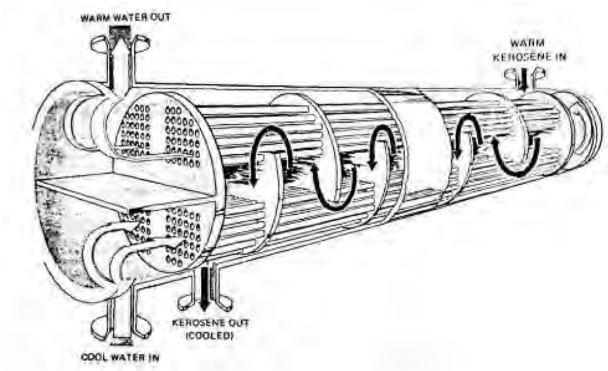

Figure 2.9: Fixed Tube Sheet (Escoe, 1986)

The opposite of the fixed tube sheet is the Floating head. The main different between fixed tube sheet and floating head is the removability of bundle tube. The significant feature of one tube sheet is that it is "float" in shell or with shell. Floating head is best applied for extreme usage such as oil refinery and can be used for high temperature differentials of liquid of 200^{o}F and above. However, there are some part which need to be taken notes of which is the internal gasket will cause leaking and corrosions on shell. (Escoe, 1986).

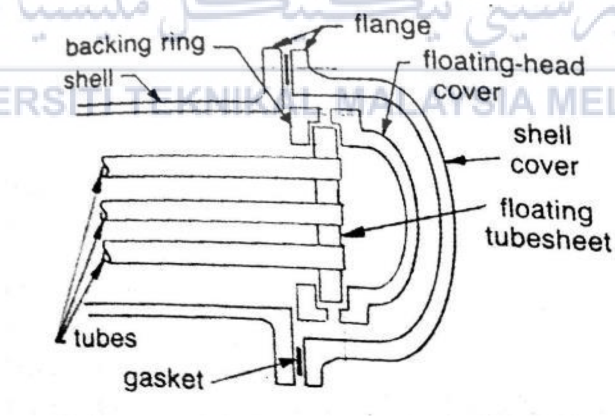

Figure 2.10: Floating Heat Exchanger (Escoe, 1986)

Next is the U-tube or U-Bundle SNTHE. This type of SNTHE only required one tube sheet and the most key features is the tube bent in u shape. U-tube SNTHE is used for high temperature gap so during expansion of the fixed tube unit's precision is needed. These kinds of tube are easier to be cleaned for the tube side and shell side. However, bends must be carefully done to prevent the tubes from mechanically damage and rupture. Not only that, tube side velocity will cause erosion at the bend part of the tube. Plus, the fluid must be free of suspended particle to prevent blockage (Escoe, 1986).

Kettle SNTHE is similar to U-tube SNTHE. The only difference is the kettle SNTHE shell is enlarged to allow boiling and vapour release. The enlarge shell has allow the SNTHE to perform vaporisation and condensation. However, this device can only be mounted horizontally and it is larger compared to other type of SNTHE (Escoe, 1986).

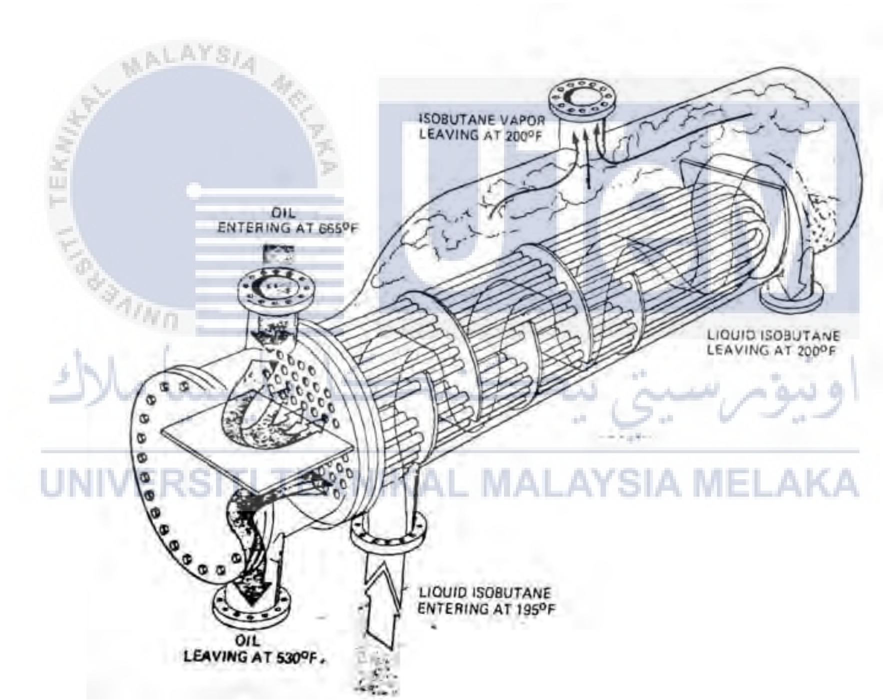

Figure 2.11: Heat exchanger with kettle and U-tube (Escoe, 1986)

2.3 Flow Condition

According to Cengel and Cimbala (2010), fluid is a substance that may exist as liquid or gas. When fluid relates to mechanic, it will be the science of fluids behaviour in rest or in motion of two different interacting fluids at the boundaries. Cengel have categorized the type of fluid flow conditions; compressible flows versus incompressible flows; internal versus external flows; laminar versus turbulent; natural versus forced flows; steady versus unsteady flows; one-, two- and three-dimensional flows and viscous versus inviscid regions of flows.

2.3.1 Viscous Versus Inviscid Regions of Flow.

When two fluid layers move near to each other, frictional force is produced and the slow layer fluid will try to slow down the fast layer fluid. This internal resistance flow or a measure of internal stickiness of fluids is known as viscosity. Viscosity occurred because there is a cohesive force between the fluids molecules or molecule collision in gases. Viscous flow occurred when there is a significant effect of friction happened. However, for region far from solid surfaces, the viscous forces are very small compared to inertial or pressure forces. So by removing the viscous term, the analysis is simplified without much loss in accuracy; it is called the inviscid flow (Cengel and Cimbala, 2010).

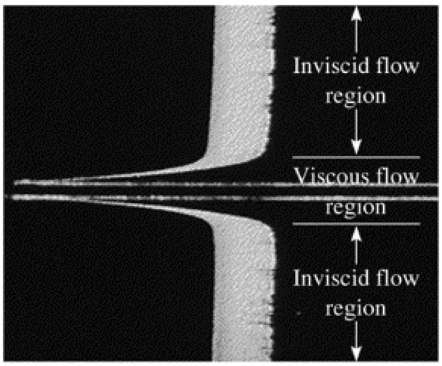

Figure 2.12 : Illlustraion of Viscous and Inviscid Flows (Cengel and Cimbal, 2010)

The study of viscous and inviscid region of flow is done by inserting a flat plate parellel to a fluid stream of uniform velocity as shown in Figure 2.12. From the figure, it is observed that the fluid stick to the both sides of the plates. This is because of the no slip condition and the thin boundary layer, the viscous effect is significant near the plates surface which is define as the viscous flow region. However, the flow region on both sides far from the plates are not affected by the plates presence. This is inviscid flow region (Cengel and Cimbal, 2010).

2.3.2 Internal versus External Flow

The fluid flows are categorized as internal and external flows depend on the flow space whether the fluid flows in a small space or over a surface. External flow is the flow of an unbounded fluid over a surface such as a plate, a wire, or a pipe while internal flow is fluid flow bounded completely by solid surfaces. For example, water flow in a pipe or duct is internal flow while airflow outside a pipe is an external flow. Usually, internal flows are greatly affected by viscosity through the flow field while external flows are affected by the viscosity too but only confined to boundary layer close to solid surfaces and downstream body (Cengel and Cimbal, 2010).

2.3.3 Compressible versus Incompressible Flow

Compressible flow and incompressible flow are defined based on the density variation during fluid flow. Incompressibility is an approximSation of constant density throughout the flows. Hence, during incompressible flow, the volume of the fluids remains unchanged over the course of motion. Liquids are most of time referred to as incompressible substance as their density do not change and remain constant. For example, density of water at 1 atm change for about one per cent when a pressure of 210 atm is applied, however for gases, a pressure change of 0.01 atm will cause the density to change up to 1 per cent. This shows that liquids are incompressible fluids while gases are compressible fluids (Cengel and Cimbal, 2010).

2.3.4 Laminar versus Turbulent flow

Flows can be smooth and orderly and sometimes rather chaotic and out of order. The highly-ordered fluid motion which is also known as smooth layer of fluids is called laminar. Laminar is defined as adjacent fluid particles movement together in 'laminae'. For example, laminar flow is high viscosity fluids flow such as oil at low velocity.

Highly disordered fluid motion which flow at high velocity is characterised as velocity fluctuations and is called turbulent. For example, low viscosity fluid flow at high velocity is considered as turbulent. However, there are flows which will alternate between laminar and turbulent, it is called transitional layer. Osborne Reynolds (1880) had conducted experiments that has established the dimensionless Reynolds number, Re, which the standard characterisation of laminar, transitional and turbulent flow. Subramaniam (2003) explain the flow characteristic can be define using the equation in (2.1)

$$Re = \frac{\mathrm{v}_{avg}}{v} = \frac{\rho \mathrm{V}_{avg}\mathrm{D}}{\mu} = \frac{\rho \mathrm{D}}{\mu}\left\{\frac{\dot{m}}{\frac{\rho\pi D^2}{4}}\right\} \tag{2.1}$$

The terms *D, V*, ρ, μ, $\dot{m}$ and v refer inner diameter of the tube, average velocity of the fluid, density of the fluid, mass flow rate and dynamic viscosity.

As,

$$\dot{m} = \rho\dot{Q} = \rho\frac{\pi \mathrm{V} D^2}{4} \tag{2.2}$$

Hence,

$$RE = \frac{4\dot{m}}{\pi\mu \mathrm{D}} \tag{2.3}$$

Based on the Reynold number formula, the calculated value can be used to determine the type of flow. For commercial circular tube, when Reynolds number is less than 2300, laminar flow occurs. For transition flow, the Reynold number is in the range of between 2300 and 4000. As for the turbulent flow, the Reynold number is more than 4000 (Subramaniam, 2013).

2.3.5 Natural versus Forced Flow

A flow can be natural or forced, depend on fluid initiation method. For forced flow, an external work is done upon fluids by means of pump and fan. Well for natural flows, fluid motion occurs naturally, for example buoyancy effect, which stated that at warm condition, the fluid properties will become lighter, and thus the fluid will rise; at cold condition, the fluid properties will become denser, and thus the fluid will fall (Cengel and Cimbala, 2010).

2.3.6 Steady versus Unsteady flow

Steady and uniform flow are of the two terms that are frequently used in engineering field especially in fluids mechanics textbooks. According to Cengel (2010), steady flow is interpreted as flow with no change of properties, temperature, velocity, etc., with respect to time. For unsteady flow, it is the opposite of steady flow.

Usually unsteady flow and transient flow are used mutually but there are not the same. For unsteady, it is referred to as flow that is unsteady and not-uniform. Transient flow is normally used for developing flow, for example, the fire up of rocket engine which consists of increasing pressure that build up in the rocket engine and accelerating flow. This transient effect will occur until the engines settle down and run steadily.

Steady-flow conditions are used to describe the continuous operation of devices such as boilers, condensers, heat exchanger, turbines and pumps. These continuous operating devices are known as steady-flow device. Although the flow field near the rotating blades of turbo machine is unsteady because their properties change from point to point within device, but when considering only the overall flow field of the devices, any fixed point of the device will remain constant. The fixed point of the device will include the mass, total energy content of a steady-flow device and volume. However, cyclic devices like reciprocating engines and compressors do not satisfy the steady-flow conditions as different and pulsating inlet and outlet flows. These devices can be considered as steady-flow when the fluid properties vary periodically (Cengel and Cimbala, 2010).

2.3.7 One-, Two-, and Three-Dimensional Flows

Flow field can be justified using velocity distribution. When flow is stated to be one-, two-, three-dimensional, it is referring to the flow velocity that is varying in one, two, or three primary dimensions or directions. Usually, fluid is a three-dimensional fluid flow phenomenon which involving x, y, z axes in rectangular coordinates and r,θ, z axes in cylindrical coordinates but velocity variation are relatively small in some regions compared to main direction of flow resulting to the small velocity variation can be ignored with diminish error. Hence, flow can be modelled as one- or two-dimensional which will make the analysis more convenient and easier to be analyse.

Considering the fluid flow from tank to circular pipe, the fluid velocity on all the pipe surfaces can be considered zero at no-slip condition and the two-dimensional flow at the entrance region of the pipe which is in r and z directions. As the velocity profile developed and steadied, it is known as fully develop region. A fully develop flow is one-dimensional as the flow only change in one direction (Cengel and Cimbala, 2010).

2.4 Flow Characteristic in SNTHE

Diaper and Harper (1990) measured velocity distribution of bypass lane using experimental technique. From the velocity measurements in the bypass flow region, bypass flow fractions are identified. Gupta and Katz (1957) also had pictured the shell side flow by using a tracer particle in a small glass cylindrical exchanger. However, the validation of result was limited to a small-scale model in a 152.4 mm shell with 26 tubes. Later, Berner et.al (1984) experimented on the fluid flows at the baffles insides the cross section of Plexiglas rectangular shell. The flow is visualised by dye injection and aluminium tracer particles. Perez (1984) used oil-lampblack technique to visualize a 101.6 mm cylindrical shell side flow which contains 92, 6.35 mm tubes. Later on, Murray (1988) has replicated the studies and formed detailed studies of shell side flow by using dye injection technique. He found a large pressure drop in the baffle area and concluded that cross-flow velocities are not uniform (Pekdemir et al., 1993).

Pekdemir et.al (1993) concluded that increased distance of upstream and downstream baffles will increase cross-flow variation but this can be reduced with radial distance of central vertical plane between tube bundle and shell wall. Highest cross-flow velocity is observed at the centre of the tube bundle around the downstream of the baffle. The recirculation zone at the baffle edge proves the existence of low velocity.

Pekdemir (1993) also made a pressure-drop measurement in the shell side flow and concluded that cross-flow pressure is related to Reynolds number. At low Reynolds number, constant pressure distribution is observed. At higher Reynolds number, cross-flow pressure variation is big with respect to the baffles distances. The pressure of cross flow is observed around the central plane (Pekdemir et al., 1993).

Zukaukas (1972) generalized the dependency of Reynolds number on the tube pitch characteristics of a tube bundle. Wilson (2000) used calculation to predict the pressure drop and heat transfer characteristics. Mandhani (2002) experimented the heat transfer characteristics for an incompressible, steady cross flow over a tube bundle and suggested the Nusselt numbers in terms of the Reynolds and Prandlt number over a range of tube banks gap. Khan (2006) had developed an analytical model with steady, laminar and fully developed flow to investigate the heat transfer for tube banks in cross flow under isothermal boundary conditions. Kim (2013) used ANSY FLUENT to figure out the flow and heat transfer characteristics of inline tube banks and suggested a correction point based on Zukaukas paper on the relationship of longitudinal pitch effect towards the flow and heat transfer rate. Li (2014) had done a fluid simulation of the fluid flow and heat transfer in one of line tube bundle wall. The local and average flow and heat characteristics is analysed and the trends of the fluid flow is identified at different impacting angles. At the same mass flow rate, the values of parallel velocity components in different shell sides are the same however the vertical velocity is different. Li concluded that the thermodynamics performance of the shell side depends greatly on the vertical component fluids velocity (Wang et al.,2016).

Gillea et.al (1971) have used Laplace transform of the exit temperature to the laplace transform of the inlet temperature and flow rate is related with mean of the transfer equation. Azilinon (1988) used the two-parameter method in the case of double pipe heat exchanger when inlet flow rate of one fluid is submitted to a step of flow rate. Guellal (1993) extend the two-parameter method by using two inlets simultaneously to identify a flow rate. Wakil et.al (1995) extend the studies of Azillion and Guellal further by manipulating the flow rates of the inlet. Lachi (1996) later extend the research by varying the inlet flow rates simultaneously to understand the behaviour of the fluid flow in the Shell and tube Heat Exchanger (Lachi et al., 1996).

2.5 CFD in Shell and Tube Heat Exchanger

Computational fluids dynamics (CFD) have been widely used as the development of the computational power have increased as the technology modernised. From the published literature, CFD have been widely used to understand the flow patterns inside the Shell and Tube Heat Exchanger (SNTHE) in order to speculate SNTHE performance on mixing, heat transfer, gas induction and solid suspension (Pal, 2016).

Prthiviraj et.al (1999) developed a 3D design of a baffled SNTHE. The design is based on distributed resistance method along with volumetric porosities and surface permeability. A single computational cell will have some multiple tubes; hence, the mesh can be done coarsely. This simulation has achieved agreement between experimental and analytical result which CFD predictions of pressure drop and temperature field are within 7.4% and 15%. Yongqing Wang et.al (2007) simulated that the heat transfer coefficient is 10 % different and pressure drop for 20%. Qiuwang Wang et.al (2008) used ANSYS Fluent for SNTHE simulation. GAMBIT was used to mesh and the solution method is SIMPLE. However, overall heat transfer rate drops 8.4% and the pressure drop 3.6%.

According to Kim et.al (2008), ANSYS FLUENT 6.0 was used to run the simulation. The mesh used is tetrahedral and the model is k- ε turbulence model with SIMPLEC as the solution method. After the simulation, Myoung conclude that a good agreement is observed when compared experimental and simulation results (Aslam et.al (2012).

Wang et.al (2009) investigated overall heat transfer rate and the pressure drop through shell side with helical baffles using ANSYS FLUENT and good agreement have been achieved between CFD result and experimental data. Koorosh Mohammmadi et.al (2009) analysed using ANSYS FLUENT 6.1. The mesh is done using hexahedral with 1200000 cells. K- ε with RNG method is used for the turbulence model and Pressure-Velocity Coupling Scheme, SIMPLE is used. Ender Ozden et.al (2010) consider simulation of the small size SHNTE as commercial SNTHE have leakage baffle flow and bypass flow which will complicate the shell side flow. ANSYS FLUENT 6.3 is used as the operating software. Two types of meshing is done, quadrilaterals and tetragonal hybrid with element of coarse cells of 70000 and fine cells of 1360000. Simulation is performed with standard k-epsilon model, 2nd order K-epsilon model, and realizable K-epsilon and Spallart-Allmaras turbulence models. The baffle used range from 6 to 12 baffles and the heat transfer was evaluated by log mean temperature difference (LMTD) with the result obtain from temperature profiles obtained from simulations. Ozden focus on the effects of several types of baffles and their cut, spacing on pressure drop and heat transfer. He concluded that the CFD results overestimated the analytical results by 36%. Anthony et.al (2011) simulated the SNTHE case with ANSYS FLUENT and using GAMBIT as the meshing tool. K- ε model is used and Second Order Upward Scheme is used for discretization. The simulation method used PISO for the Pressure-Velocity Coupling Scheme.

Bhutta et.al (2012) reported numerous studies of CFD simulations in the field of heat exchanger focusing on flow maldistribution, fouling pressure drop and heat transfer. While Zheng and Zhang (2012) studied about the effects of length to diameter ratio of a SNTHE on fluid flow maldistribution and heat exchanger performances. Bhuta proposed that further studies on the same problem can made by using a multi parallel channel inlet and outlet.

According to Wang et.al (2016), a tubular heat exchanger is used. The outside diameter of the tube is 25 mm. The tubes are arranged in staggered layout with tube pitch of 32 mm. There are 10 rows of tubes arranged along the fluid flow and each row contain 10 tubes. The whole model width is 320 mm, thickness 200 mm and height 600mm.

For the Setup of fluent solver, the fluid is liquid water and it flow in *x*-axis direction. The inlet is set as velocity-inlet with the bulk temperature of fluid as 29.15K with pressure outlet of 0Pa. The side faces of *z*-axis are symmetrical from front to back face and *y*-axis are set as the adiabatic and stand non-slip wall conditions. Tube surface are set as stand non-slip wall conditions with constant temperature of 283.15K (Wang et.al, 2016).

For the meshing of 20,000 Reynolds number, the number of grids ranges from 8,356,500 to 2,500,000 with less than 1% difference for of Nusselt number and pressure drop Reynold number use is 20,000 (Wang et.al, 2016).

Using FLUENT, specific volume method on a collocated grid is used to analyse the fluids problem. Numerical simlations perfomed with three-dimensional, steady-state, and turbulent flow system. K-esiplion was used for the viscous model and enegy equation is incuded, SIMPLE algorithm second-order upwind scemes and pressure-velocity coupling was used to discretize the momemtum and energy equations (Wang et al., 2016).

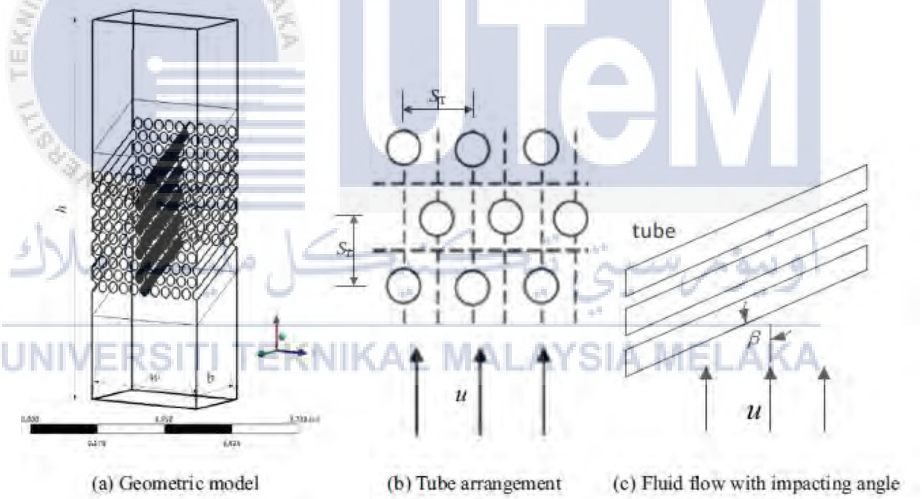

Figure 2.13 : geometry of tubes (Wang et.al 2016)

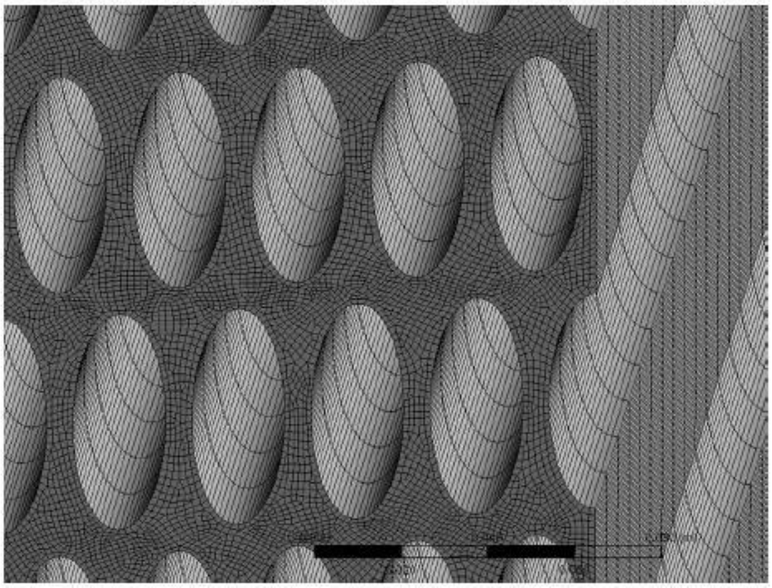

Figure 2.14 : meshing at the tubes (Wang et.al 2016)

CHAPTER 3

GENERAL METHODOLOGY

3.1 Introduction

In this section, the method to carry out this project is discussed. Throughout the project, the objective and the scope were constantly referred, to ensure the method is relevant to the objectives and scopes. The computational domain was identified based on the journal. Then, the model is built using ANSYS Design Modeler and mesh is applied on it. Solver is set up according to literature review. Constraints were checked and then validated to ensure the result is trustworthy. The boundary condition is changed too in order to understand more about the flow condition in Shell and tube Heat Exchange (SNTHE).

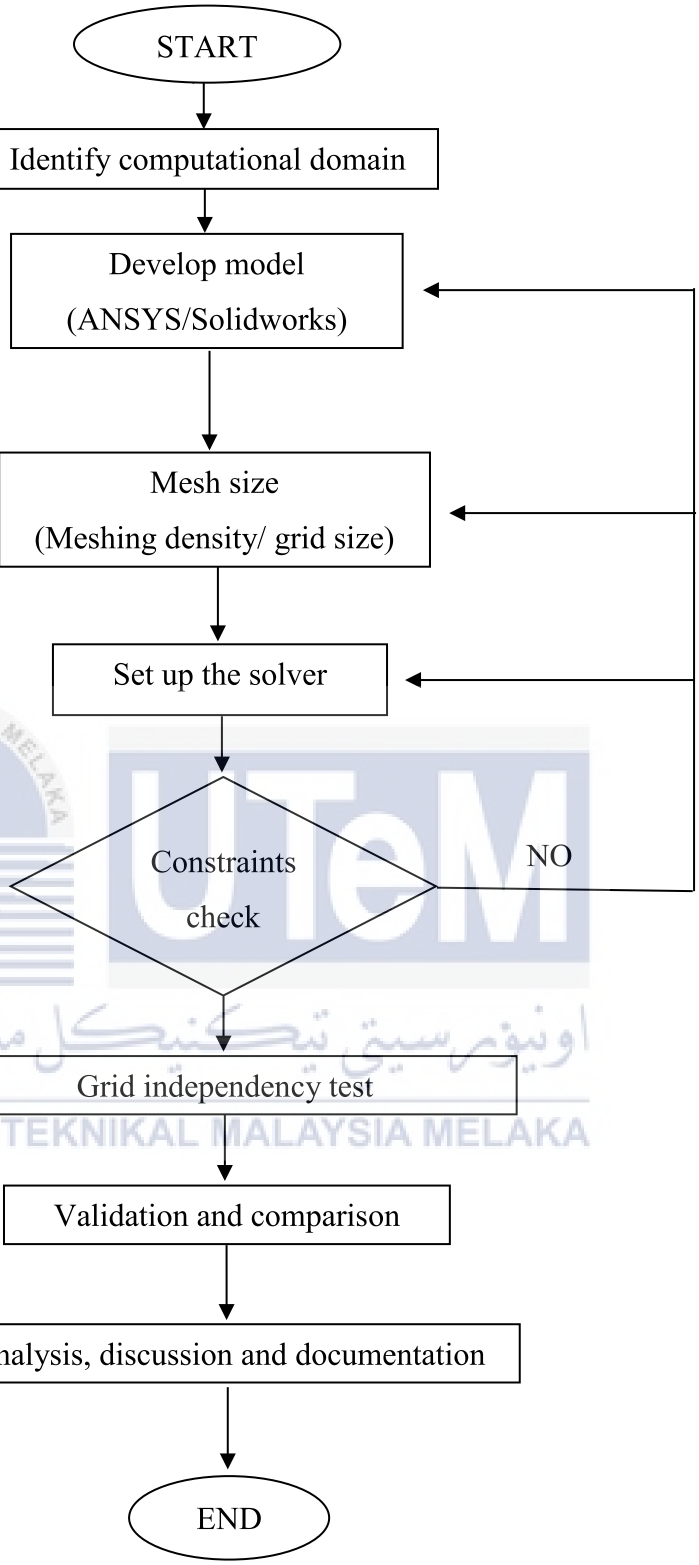

Figure 3.1: Flow chart

3.2 Geometry

For the geometry, Shell and Tube Heat Exchanger (SNTHE) without baffle is chosen as the domain. The un-baffle SNTHE is used because the presence of the baffle will affect the flow condition of the fluid inside the shell. Baffle main purposes is to support the tubes and increase fluid velocity and heat exchange rate. However, when baffle SNTHE is used, the fluid flow is more complex and unpredictable sometime. So, un-baffle SNTHE is used as the geometry to simplify the flow inside the shell.

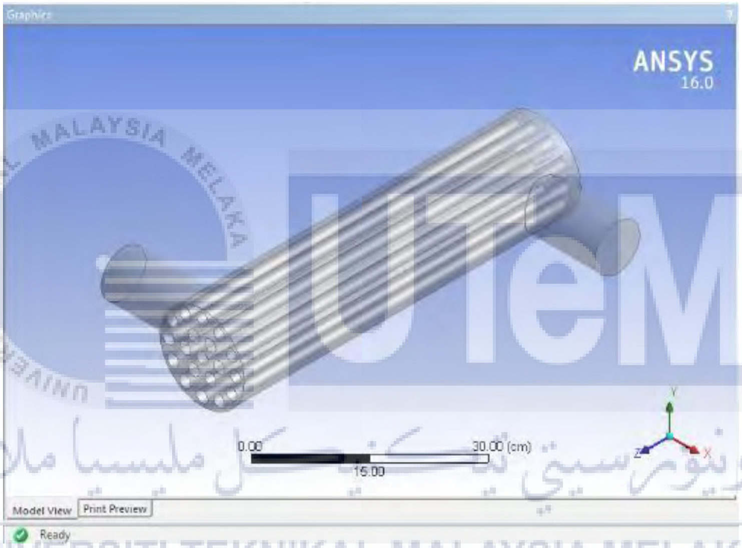

Figure 3.2 Geometry of un-baffle SNTHE

Both the inlet and outlet diameter of the SNTHE are set as 7.98cm. to let the outlet flow fully developed, the outlet length is designed longer. The shell diameter is 15 cm and the tube diameter is 2 cm. The length of the shell is 60 cm. There are 19 tubes in the shell with pitch distance of 2 cm. This domain is set up based on Kim and Aicher (1997) model which Pal et al. (2016) cited that this model was used to compare their results with the experimental results on actual SNTHE model.

For this project, only one geometrical model will be used as the flow condition of SNTHE is the main objective in this project. Hence, the model will not be changed and only the boundary condition will be changed based on the validated setting.

3.3 Mesh Generation

The meshing used for this model is a 3D tetrahedron meshing. Tetrahedron is used as it can create cells with more nodes where more points are simulated. This gave a better and more accurate results. Inflation is applied on the tube wall and the shell wall to investigate the boundary layers on that area. Mesh size of 350000, 700000 and 1100000 cells is created for grid independency test (Pal, 2016). However due to licence limitation, mesh size of 350000 is used. After that, the wall will be defined in order to set the boundary condition during the solver stage. From Figure 3.3, the wall will be labelled as inlet, outlet, tube wall and shell wall.

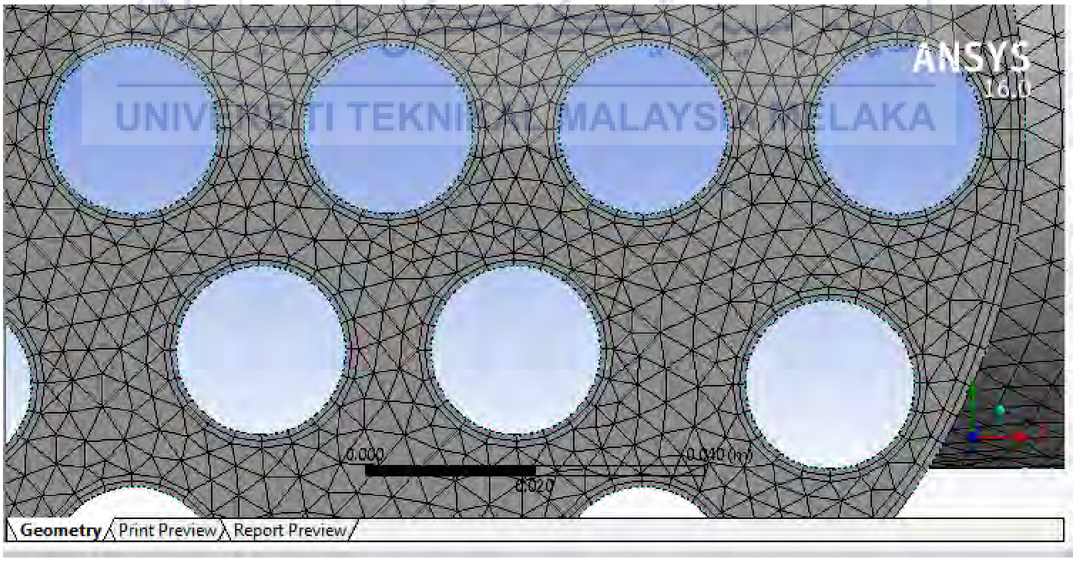

Figure 3.3 Mesh with Tetrahedron and Inflation.

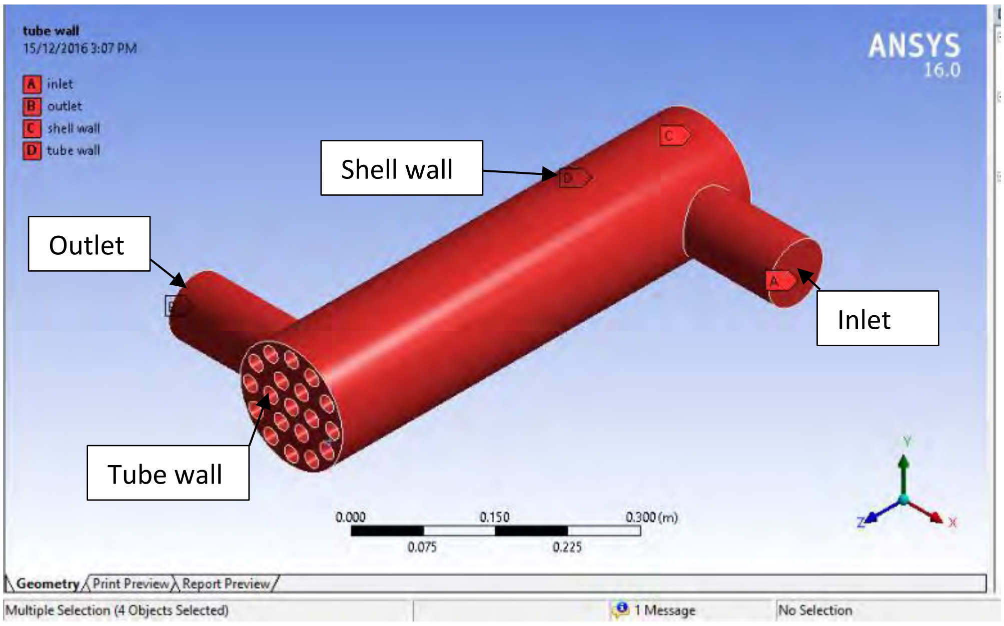

Figure 3.4 Wall selection

3.4 Solver Setup

3.4.1 Assumption

Before setting up, few assumptions were made. The flow is assumed as incompressible fluid flow as the density remain constant throughout the process, no phase change will occur and no chemical reaction takes place. Constant mass flow rates inlet condition is used at the inlet boundary condition. The flow is also assumed as steady and continuous (Pal, 2016).

3.4.2 Boundary condition

` The inlet is set as mass flow rate inlet following the statement of Pal et al. (2016) which cited that Kim and Aicher (1997) performed the simulation by varying the mass flow rate. So, the same approach is used for validation purposes. The inlet temperature is set as 30°C and the tube wall is set as no-slip wall boundaries as it is the standard for the static walls with temperature 450K. Pressure is set as pressure as the rate of change of pressure is constant.

3.4.3 Solver

For this simulation, energy equation is on as it is temperature dependent. As for the viscous model, k-ε is used. Initially, it is assumed that the inlet flow is robust and the computational time is faster compared to another turbulent model. For pressure-velocity coupling, SIMPLE is used as the flow is assumed incompressible flow (Pal, 2016). The discretization scheme is started out with first order as it is easiest to converge. However, it is advisable to run again with other type of scheme as the flow may have the potential to be not aligned with the grid. For the convergence criteria, the total converge limit is set as 10^{-7}. According to Pal (2016) he cited that Uzzan et al. (2004) found out the temperature remains constant with variation 0.01% at the residual value below 10^{-7} (Pal, 2016)

CHAPTER 4

RESULT AND DISCUSION

4.1 Overview

Validation is done to check the reliability of the model design. Validation is done by comparing the outlet temperature, heat transfer rate, mass flow rate, Reynold Number and heat transfer coefficient.

Using the validated model, three types of fluid are studied; Ammonia, Isobutane (R600a) and Carbon Dioxide. Flow contour, temperature contour, velocity distribution and temperature distribution are analysed using Ansys Fluent. These fluids have properties taken at 30°C as shown in Table 4.1.

Table 4.1 Fluid properties of Ammonia, R600a and Carbon Dioxide

	ρ, kg/m^3	C_p, J/kg.K	k, W/m.k	μ, m^2/s
Ammonia, NH_3	1167	4828	0.4695	1.361×10^{-4}
Isobutane, R600a	544.02	2492	0.0935	1.434×10^{-4}
Carbon Dioxide, CO_2	1.84198	844.36	0.016972	1.5172×10^{-5}

4.2 Grid independency test and Validation

Due to license limitation, the model of mesh size 350000, 400000 and 450000 is used for grid independency test. The solution is converged under the convergence criteria set by Pal (2016) with velocity at 10^{-4} and energy at 10^{-7}. From the simulation, the result is recorded and tabulated in Table 4.2.

Table 4.2: Grid Independency Test Result

Mesh Size	Mass flow rate, kg/s	Outlet temperature, K	Outlet velocity, m/s	Heat Transfer Rate, Q(kW)	Heat Transfer Coefficient (W/m^2K)	Reynold Number	Nusselt Number
350000	0.4804	360.31	0.1064	115.18	1108.19	3125	50.45
400000	0.4805	360.02	0.1052	114.76	1101.60	3125	50.15
450000	0.4832	359.59	0.1049	114.36	1096.79	3125	49.94

Apart from ANSYS result, some calculation was made to understand the shell side flow better. The Reynolds number is calculated based on the formula cited by Pal (2016).

$$\mathrm{Re} = \frac{\rho v D_h}{\mu} \quad (4.1)$$

Where, ρ is the density, v is the inlet velocity, μ is the viscosity and D_h is the hydraulic diameter of the shell.

According to Pal (2016), density is equal to 995 kg/m^3, velocity is 0.10047 m/s, viscosity is 8.955 x 10^{-4} Pas and hydraulic diameter is equal to 0.028 m. With values above, the Reynold number is equal to 3125.

Next is Nusselt Number. According to Pal (2016), The Nusselt number formula used are;

$$Nu = h\,D_h / k \quad (4.2)$$

where, h is the heat transfer coefficient, k is the thermal conductivity, D_h is the hydraulic diameter. As the simulation run with inlet temperature of 30°C, thermal conductivity is 0.615 W/m.K where the value is taken from table of the properties of water cited by Cengel, Ghajar (2015). Heat transfer coefficient are obtained from the simulation result which 1108.19 W/m^2K and the density is 995 kg/m^3 as cited by Pal (2016).

Hence,

$$Nu = \frac{hD_h}{k} = \frac{1108.19\ (0.028)}{0.615} = 50.45$$

Table 4.3: Percentage difference

	Journal value	350000	400000	450000
Masss flow rate, kg/s	0.5	3.92	3.9	3.36
Reynold number, Re	1502	108	108	108
Outlet temperature, K	335.54	7.38	7.30	7.17
Heat transfer rate, Q (kW)	76.16	51.23	50.68	50.16
Heat transfer coefficient, (W/m^2k)	809.05	36.97	36.16	35.57
Nusselt Number	36.86	36.86	36.10	35.49

Based on the data above, generally, the percentage difference is decreasing. For the mass flow rate, the percentage error decreases from 3.92% to 3.36%; Outlet temperature decrease from 7.38 to 7.17%. Hence, this proof that when the mesh increase, the percentage of difference becomes lower. This is because as the mesh increases, more nodes are available to obtain and received data. With more nodes and more data, a more accurate result will be obtained.

As for the highest percentage difference, which is the Reynolds Number, the reason is currently undefined. The Reynolds is calculated as cited as Pal (2016), and the simulation is run based on the Pal (2016) setting. After performing the calculation and the simulation, the result does not seem to change very much. Apart from the Reynolds Number problem, the other result is acceptable hence this model can be used for simulation. The model of mesh size of 350000 is used as it is easier to be compared to the result in the journal paper.

4.3 Ammonia

Ammonia has been environment friendly and cheap natural refrigerant for a century and more. According to Zahid et.al (2016), Ammonia is limited due to its toxicity and flammability but when used under a well-designed heat exchanger, it will be an alternative as it has higher specific heat capacity than water.

4.3.1 Ammonia Flow Contour

Figure 4.1 shows the flow contour at inlet (z/L = 0.1). Here we can see that at point A and point B, there is only slight backflow of the fluid as the fluid around the bottom of the shell. This is due to the flow at inlet is slightly higher, which is around 0.15 m/s, hence, resulting the fluid around the shell to continue flow through the tubes. From Figure 4.2, the flow contour at central plane showed that fluid flow at the bottom part of the shell are slightly faster than the top part of the shell. This phenomenon occurs because the existence of gravity effect. However, Ammonia have viscosity of 1.361 x 10^{-4} kg/ms, so the flow able to flow till to the outlet. Hence, Ammonia can penetrate uniformly through the tubes, especially at the bottom part of the shell. In this study, the term ‘fluid penetration’ represents behaviour of fluid as it flows inside the area between the walls of the tube and the shell. At the outlet, there is flow recirculation observed and this is referred as a dead zone. Although dead zone occurs, but this area does not play a significant role in heat transfer as it does not help carry out conduction between the tube and fluids.

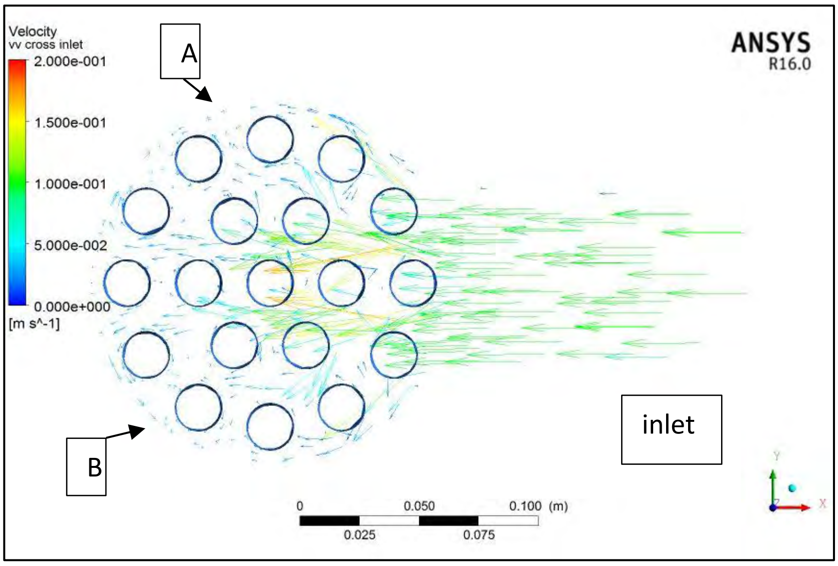

Figure 4.1 Ammonia flow contour at inlet of Shell

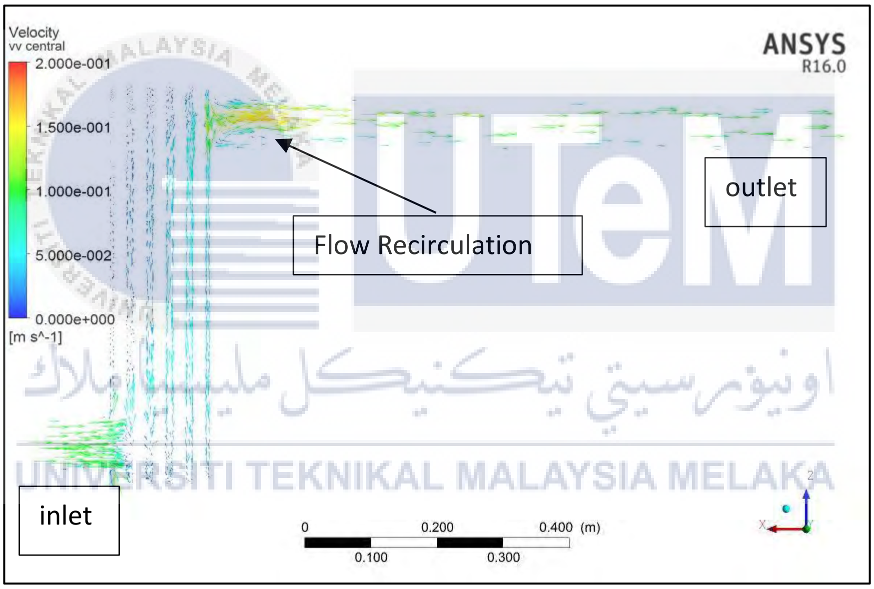

Figure 4.2 Ammonia flow contour at central plane

4.3.2 Ammonia Temperature Contour

Figure 4.3 shows the temperature contour of the fluid at inlet, outlet and central plane. From Figure 4.3(c), the flow is faster and concentrated, hence, the top region of the shell is colder. As it moves down, the flow disperse a flow along the tubes, hence, the bottom of the shell is hotter than the top part with over 320K compared to 305K. At Figure 4.3(a), we can see at inlet, the temperature is lower as cooling fluid come in in this direction. As it moves along to the tube the temperature become hotter and hotter as it cool down the tube temperature by taking away the heat in the tubes. As the ammonia have high special heat capacity and thermal conductivity, only at point c when the temperature starts becoming constant at 350K and phenomenon will continue through to the outlet. However, at the outlet, the top part of the shell has higher temperature which is 360K, as the fluid that reach the end of the shell is not as cold as the inlet fluid.

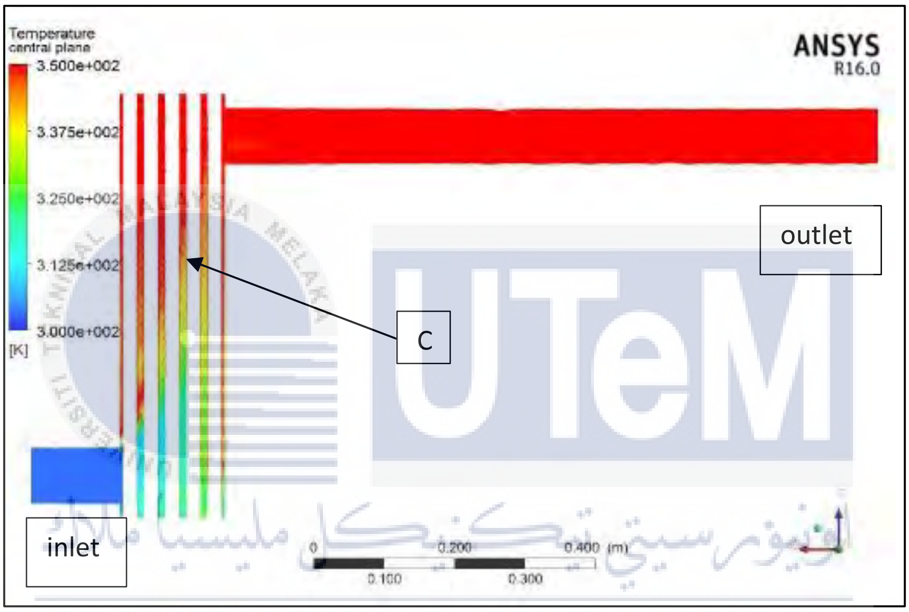

(a)

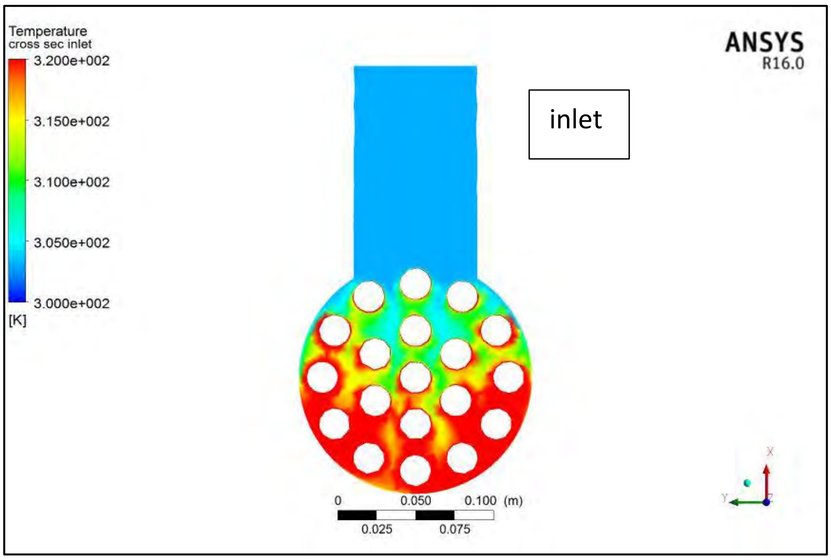

(b)

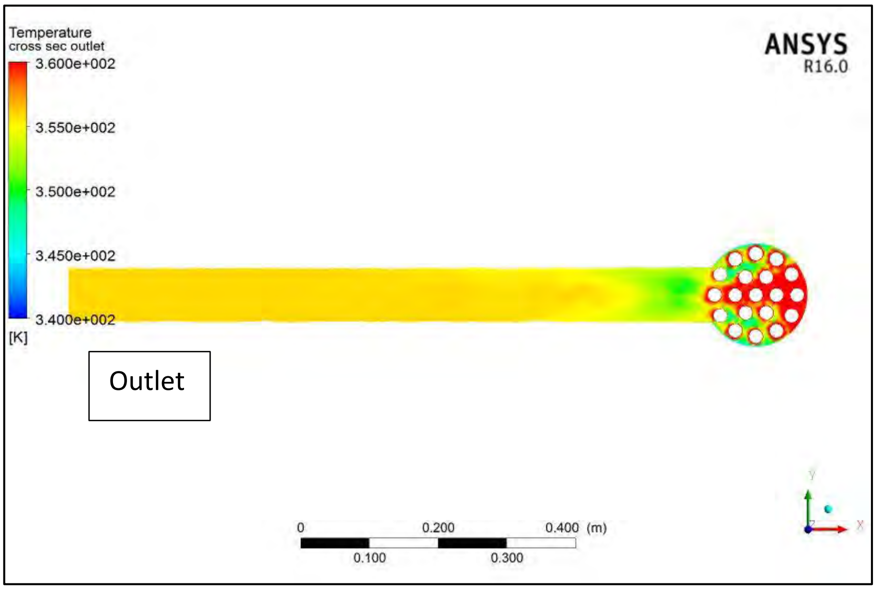

(c)

Figure 4.3 Temperature Contours of Ammonia at 3 different planes: (a) Central plane; (b) inlet of the shell; (c) outlet plane

4.3.3 Ammonia Velocity Distribution

Figure 4.4 (b) shows axial velocity that are analyse at line 1, line 2 and line 3. Line 1 is represented as 'av-inlet' at radial position z/L=0.1. Line 2 is represented as 'av-middle' at radial position z/L=0.3 and lastly Line 3 is 'av-outlet' which is located at radial position z/L=0.9. Generally, the axial velocity near the tubes are zero because of the no slip wall condition. At the 'av-inlet', the flow is low as the flow enters the shell in radial direction. At 'av-middle', the flow is converted from radial direction to axial direction. In Figure 4.4 (a), 'av-middle' is represented as red dots. It is observed from the figure that the axial flow is fully develop and the flow is stable through the tubes, hence, the fluid penetration the strongest. The maximum peak of axial flow is observed to shift toward the outlet at radial position z/L=0.9. This is due to gravity effect causing the fluid to concentrate more at the bottom of the shell. The highest fluid flow is observed at the radial position of z/L equals 0.9 with velocity of 0.0575 m/s.

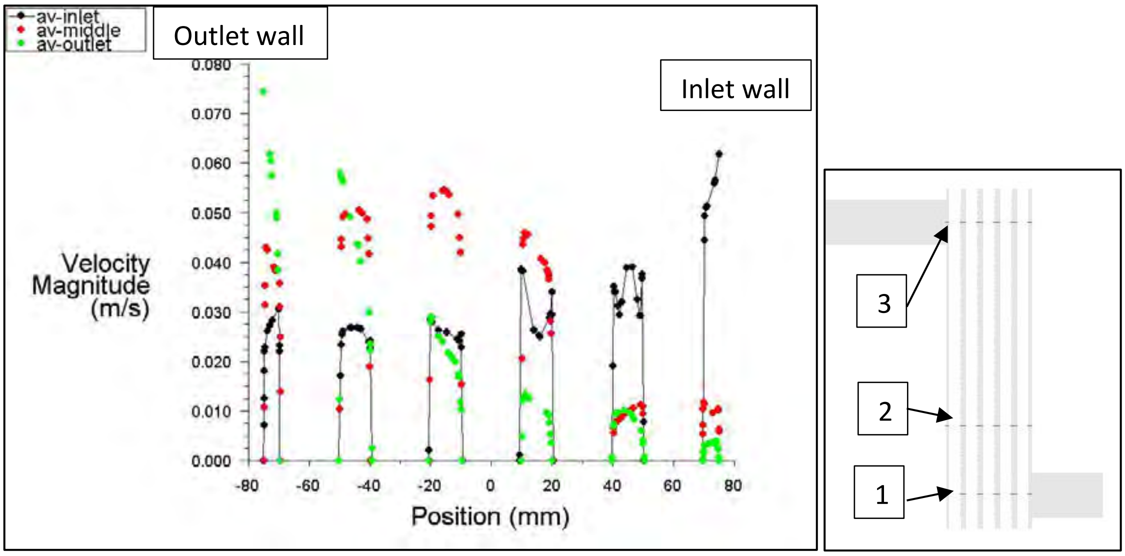

(a) **(b)**

Figure 4.4 (a)Variation of Ammonia axial velocity with dimensionless radial distance; (b) axial distance (1) z/L = 0.1, (2) z/L = 0.3, (3) z/L = 0.9

4.3.4 Ammonia Temperature Distribution

Figure 4.5 shows the temperature distribution along the radial distance of the shell. As shown in Figure 4.5 (b), 4 lines are plotted at $x/D_s = 0.2$, $x/D_s = 0.4$, $x/D_s = 0.6$ and $x/D_s = 0.8$. $x/D_s = 0.2$ is defined as 't-inlet1', $x/D_s = 0.4$ is defined as 't-inlet2', $x/D_s = 0.6$ is defined as 't-inlet3' and $x/D_s = 0.8$ is defined as 't-inlet4'. Figure 4.5 (a) shows the temperature distribution across the axial dimensionless distance of the shell which is z/L. The position of the dimensionless axial distance is as shown in Table 4.4. From Figure 4.5(a) at axial distance from 0 to 0.2, the 't-inlet1' has higher temperature compared to other region as the flow in this region is low due to the weakness of flow penetration of the fluids as the flow is changing from radial flow to axial flow. At axial region 0.2 to 0.8, 't-inlet4' and 't-inlet3' showed highest temperature raised compared to the other two lines. 't-inlet4' increased the most as the flow in this region is low due to the fluid flow shifted toward the outlet. Resulting not enough cold high Ammonia carry out cooling activity at radial distance $x/D_s = 0.8$. For 't-inlet1', 't-inlet2' and 't-inlet3', the temperature drop slightly from radial distance x/D_s 0.1 to 0.3 and increase from x/D_s 0.3 to 0.8. This phenomenon occurs because Ammonia at first can cool down the temperature at x/D_s 0.1 to 0.2 as it is cold and this showed that good fluid penetration occurred. As it moved along the radial distance, its ability to carry away heat reduce as Ammonia is getting hotter. Finally, At region x/D_s 0.8 to 1.0, due to the velocity reduction and hotter Ammonia, hence, the temperature is highest.

Table 4.4 Position of the Dimensionless Axial Distance

Position (mm)	-60	0	60	120	180	240	300	360	420	480	540
axial distance, z/L	0	0.1	0.2	0.3	0.4	0.5	0.6	0.7	0.8	0.9	1.0

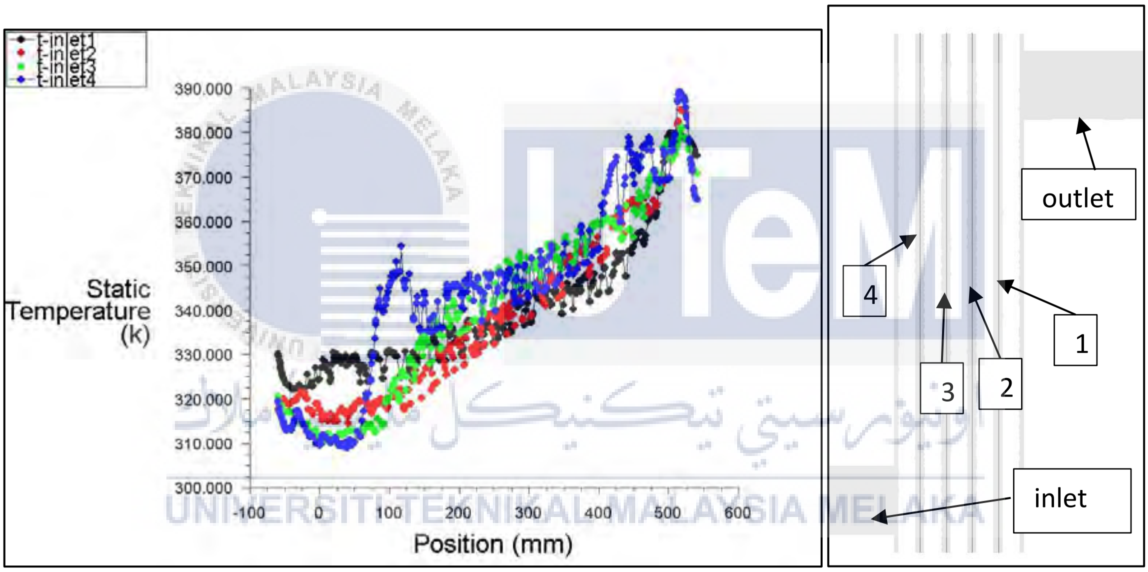

(a) **(b)**

Figure 4.5: (a) Variation of Ammonia temperature with dimensionless axial distance; (b) radial distance: (1) $x/D_s = 0.2$, (2) $x/D_s = 0.4$, (3) $x/D_s = 0.6$, (4) $x/D_s = 0.8$

4.4 Isobutane (R600a)

Isobutane is an environmental friendly refrigerant and suitable to be use on heat pump, a type of shell and tube heat exchanger variation. According Huang et.al. (2011), Isobutane is a clean and high energy efficient fluid. It also has less impact on the environment and can help to conserve the ozone layer and global warming by phased out harmful refrigerant such as R22a.

4.4.1 R600a Flow Contour

Figure 4.6 shows the flow contour at z/L 0.1, which at the inlet on the shell. It is observed that no backflow of the fluid occurred but is observed that the flow changed from radial to axial. From Figure 4.7, the flow is observed to shift towards the outlet. This occurred because of the gravity effect pulling the fluid towards the outlet. R600a have viscosity of 1.434 x 10^{-4} kg/ms, and this is relatively low, hence, constant fluid penetration across the tubes is observed. At the outlet, flow recirculation is observed, but it does not have significant effect as no significant heat transfer occurred at that position.

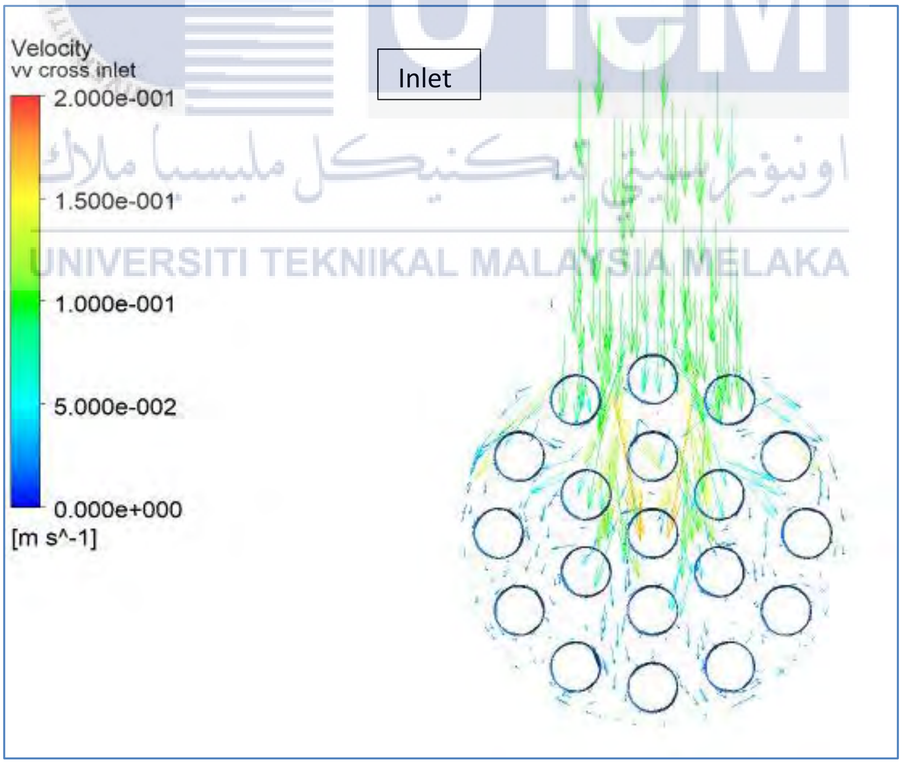

(a)

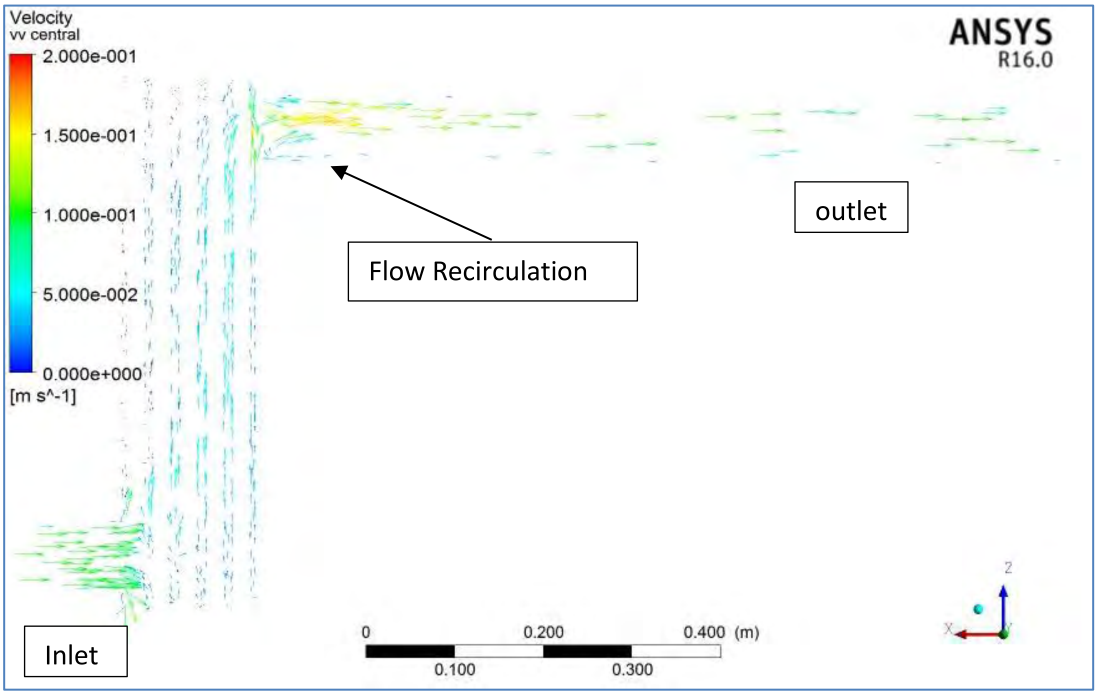

(b)

Figure 4.6 R600a flow contour: (a) inlet of the shell; (b) central plane

4.4.2 R600a Temperature Contour

Figure 4.8(b) shows the inlet temperature contour of the R600a. It is seen that at the inlet, heat transfer process is carried out smoothly as it the cool region with up to 95 % of the area has average temperature of 305K. At figure 4.8(a), the fluid temperature is observed skewed towards the outlet. This is due to the fluid flow affected by the gravity effect and resulting to skewed towards the outlet of the shell. Higher fluid temperature is observed at the end of the tubes. This showed that the fluid penetration is not enough and the cold fluid has become hot at this point. At the outlet, the temperature is separated into two regions before the temperature becomes fully developed at the outlet point. This is because of the inconsistency of the fluid penetration happening, hence, there were two different temperature regions occurred. Figure 4.8 (c) is the outlet temperature contour. Form the figure, the top part of the shell is observed to have higher temperature due to the low fluid penetration.

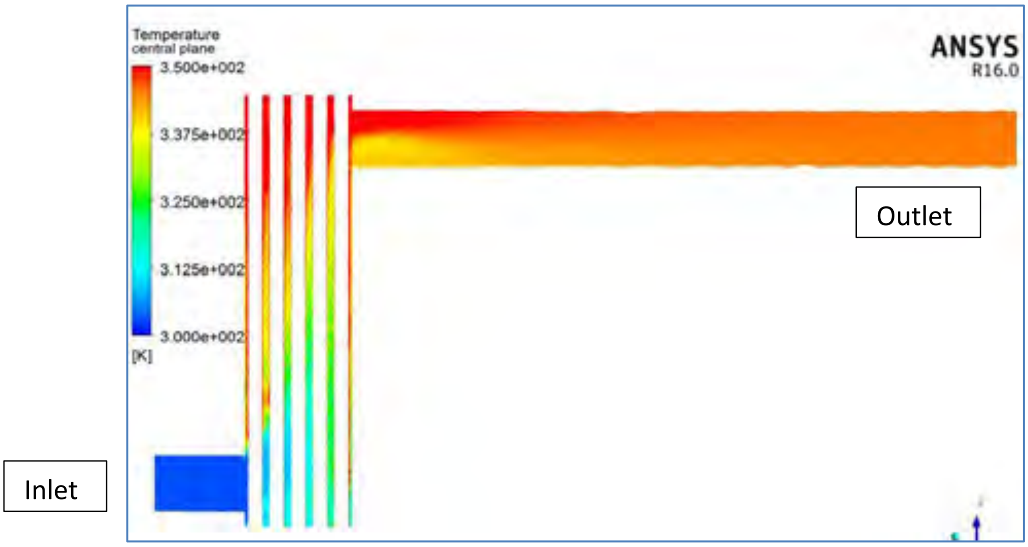

(a)

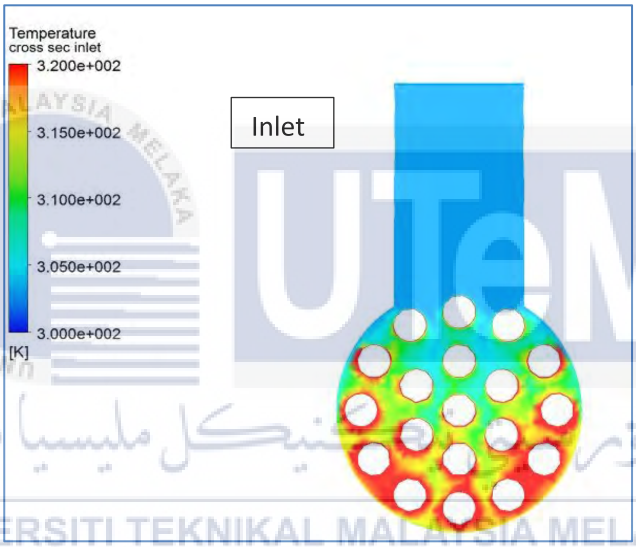

(b)

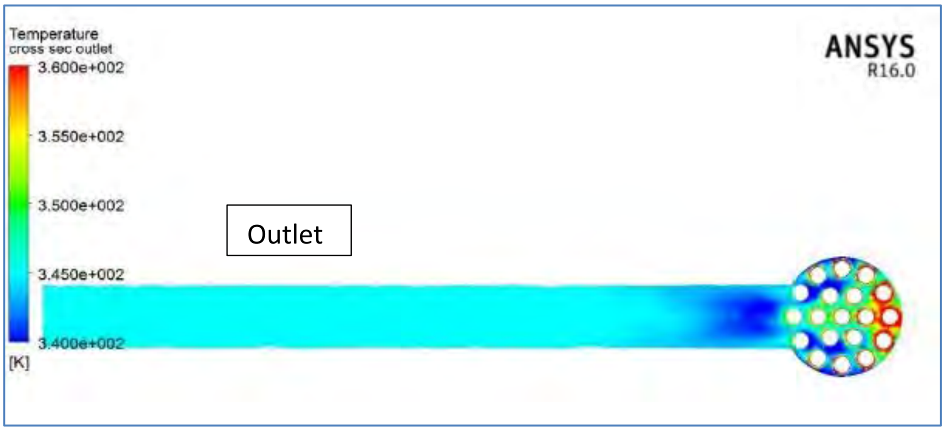

(c)

Figure 4.7 Temperature Contours of R600a at 3 different planes: (a) Central plane; (b) inlet of the Shell; (c) outlet plane

4.4.3 R600a Velocity Distribution

Figure 4.8 (b) shows axial velocity that is analyse at line 1, line 2 and line 3. Line 1 is represented as ‘av-inlet’ at radial position z/L=0.1. Line 2 is represented as ‘av-middle’ at radial position z/L=0.3 and lastly Line 3 is ‘av-outlet’ which is located at radial position z/L=0.9. Generally, the axial velocity near the tubes are zero because of the no slip wall condition. At the ‘av-inlet’, the flow is low as the flow enters the shell in radial direction. At ‘av-middle’, the flow is converted from radial direction to axial direction. In Figure 4.4 (a), ‘av-middle’ is represented as red dots. It is observed from the figure that the axial flow is fully developed and the flow is stable through the tubes, hence, the fluid penetration is the strongest. The maximum peak of axial flow is observed to shift towards to the outlet at radial position z/L=0.9. This is due to gravity effect causing the fluid to be more concentrated at the bottom of the shell. The highest fluid flow is observed at the radial position z/L=0.3 with velocity of 0.058 m/s.

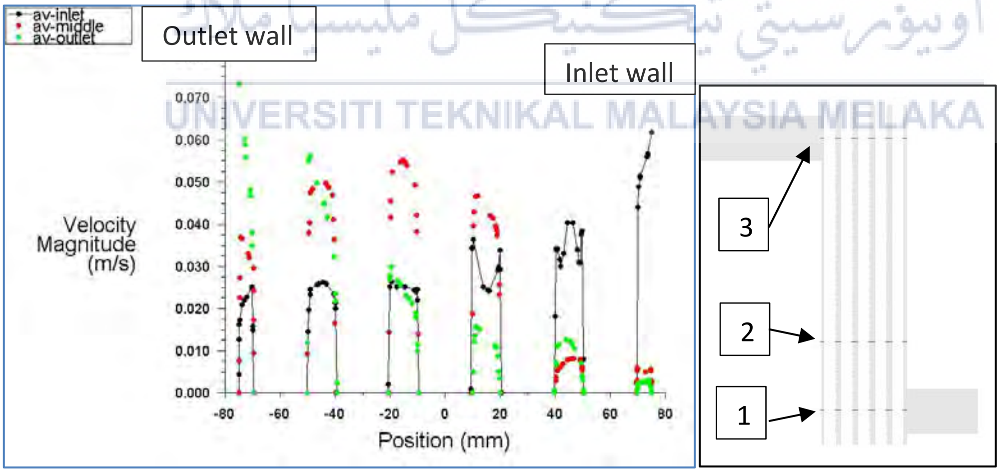

(a) **(b)**

Figure 4.8 (a)Variation of R600a axial velocity with dimensionless radial distance; (b) axial distance (1) z/L = 0.1, (2) z/L = 0.3, (3) z/L = 0.9

4.4.4 R600a Temperature Distribution

The position of the dimensionless axial distance is as shown in Table 4.4. From Figure 4.9(a) at axial distance from 0 to 0.2, the ‘t-inlet1’ has higher temperature compared to other region as the flow is changing from radial flow to axial flow. At axial region 0.2 to 0.8, ‘t-inlet4’ and ‘t-inlet3’ showed highest temperature raised as fluid flow in that area is low due to gravitational effect pulling the fluid towards the outlet. For ‘t-inlet1’, ‘t-inlet2’ and ‘t-inlet3’, the temperature increases at location x/D_s from 0.2 to 0.8. This phenomenon occurs because R600a have flow through at locations x/D_s from 0.0 to 0.2 and it has transfer the heat through convection. Hence, at the later part of the shell and tube, the temperature becomes high and fluids capability to absorb heat reduces. Finally, at region x/D_s ranging from 0.8 to 1.0, due to the velocity reduction and hotter R600a, the temperature is highest.

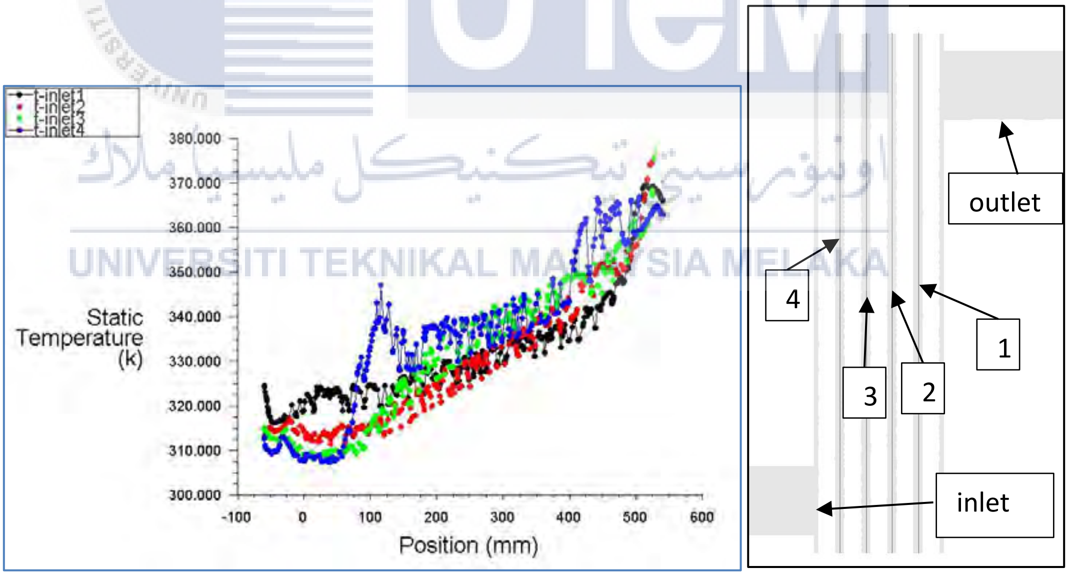

Figure 4.9: (a) Variation of R600a temperature with dimensionless axial distance; (b) radial distance: (1) $x/D_s = 0.2$, (2) $x/D_s = 0.4$, (3) $x/D_s = 0.6$, (4) $x/D_s = 0.8$

4.5 Carbon Dioxide

Claudio (2015), stated that Carbon Dioxide have the potential to be the alternatives of the cooling fluid for its environmental friendliness and high thermodynamic properties with specific heat capacity up to 1000 J/kg.K. Hence, it can be an energy efficient alternatives for tap water heat pumps, gas cooling processes or increasing the water temperature without significant changes in coefficient of performances.

4.5.1 CO_2 Flow Contour

Figure 4.10 shows the flow contour at z/L=0.1, which at the inlet on the shell. It is observed that the fluid only penetrates though the tubes near the inlet. Only diminished fluid flow at the bottom of the shell. This is due to the low density of Carbon Dioxide causing the fluid to not achieve high velocity to penetrates through the tubes. Figure 4.11 shows the flow of Carbon Dioxide at central plane. It has similar flow pattern as Ammonia and R600a with the fluid skewed towards the outlet due to gravity effect and flow circulation is observed at the outlet.

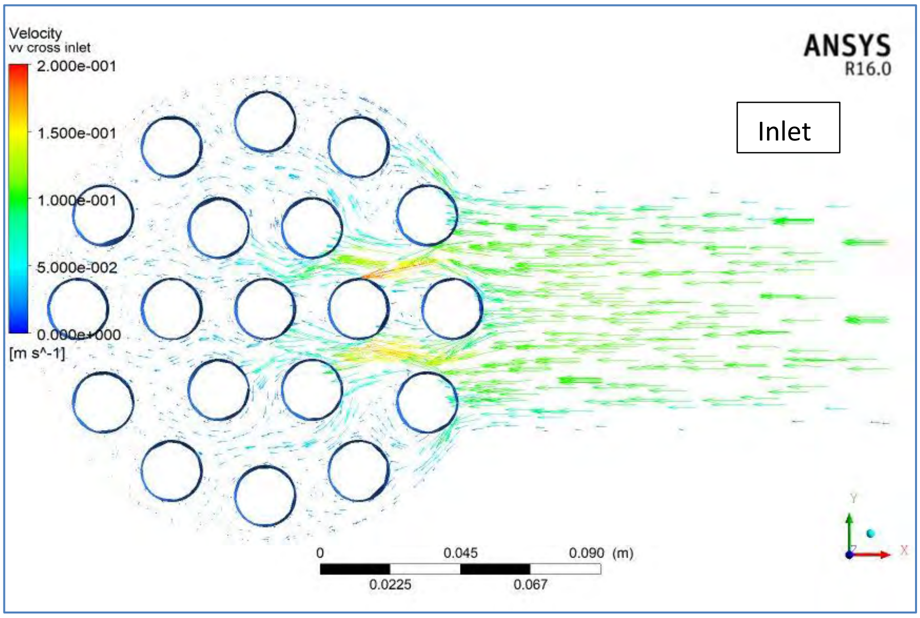

Figure 4.10 CO_2 flow contour at inlet of the shell

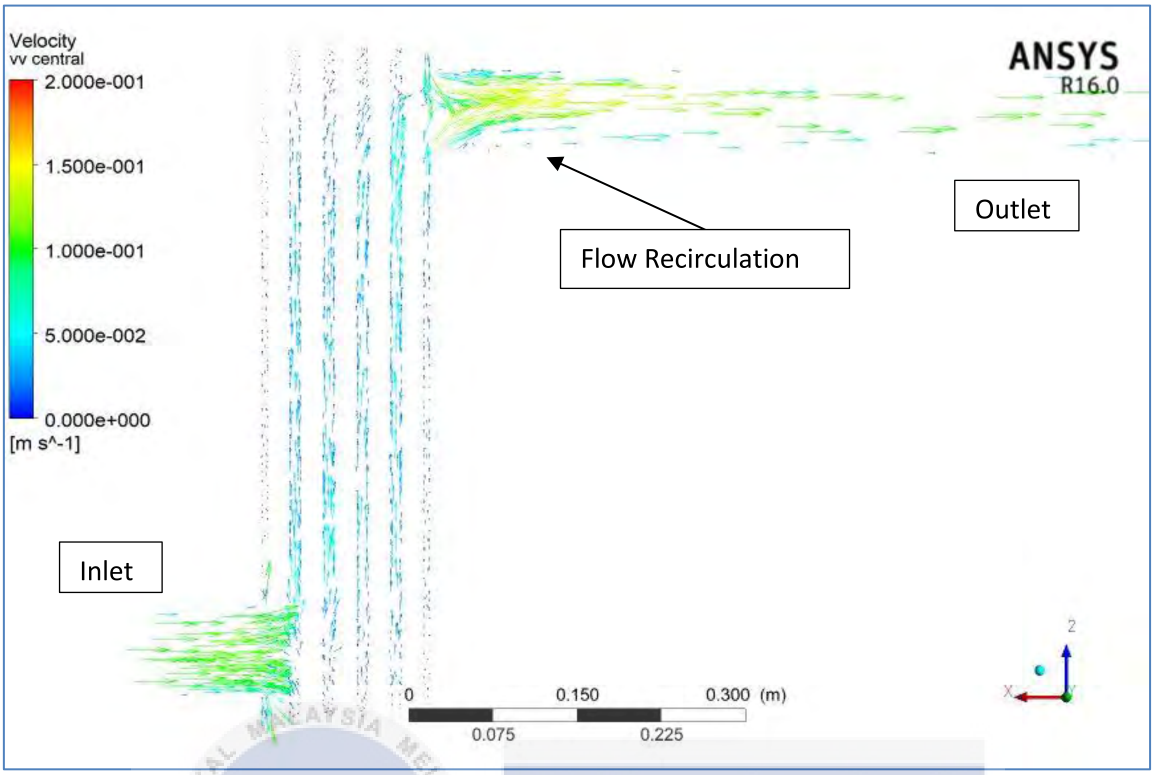

Figure 4.11: CO_2 flow contour at Central Plane

4.5.2 CO_2 Temperature Contour

Figure 4.12(b) shows the inlet temperature contour of the carbon dioxide. Due to cooling fluid used is Carbon Dioxide gas, hence, it does not show significance cooling activity. Figure 12(a) and (b) showed mostly red region indicating no significant cooling effect.

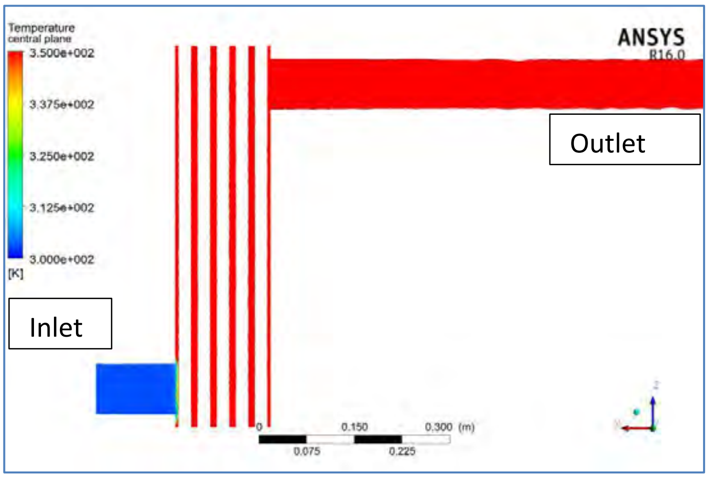

(a)

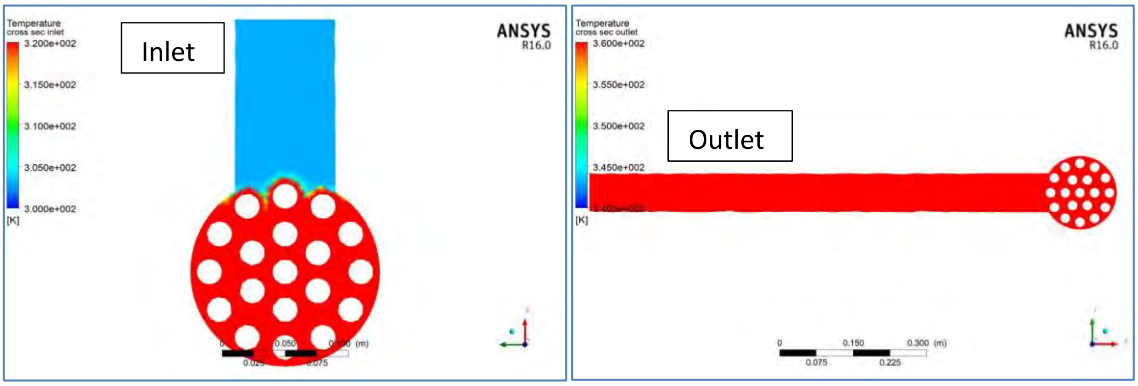

(b) **(c)**

Figure 4.12 Temperature Contours of CO_2 at 3 different planes: (a) Central plane; (b) inlet of the Shell; (c) outlet plane

4.5.3 CO_2 Velocity Distribution

From Figure 4.13(a), the line 'av-inlet' which is the line 1 at the z/L=0.1 in Figure 4.13(b), shows decreasing pattern of velocity magnitude. This due to the high velocity inlet but due to low density, it does not have enough velocity to penetrates through the tubes. At line 'av-inlet middle', axial flow velocity developed and has the highest velocity with 0.048m/s. At line 'av-outlet', the flow is skewed towards the outlet wall due to the gravity effect.

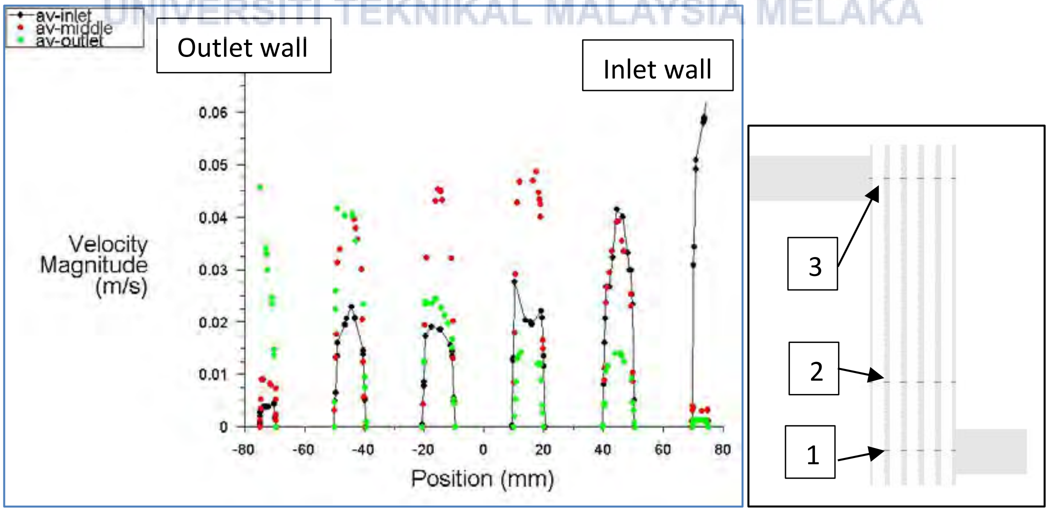

(a) **(b)**

Figure 4.13 (a)Variation of CO_2 axial velocity with dimensionless radial distance; (b) axial distance (1) z/L = 0.1, (2) z/L = 0.3, (3) z/L = 0.9

4.5.4 CO_2 Temperature Distribution

The position of the dimensionless axial distance is as shown in Table 4.4. From Figure 4.14(a) at axial distance from 0 to 0.2, the 't-inlet1' has higher temperature compared to other region as it is furthest from the inlet and the fluid penetration is weak for Carbon Dioxide. At axial region 0.2 to 0.8, 't-inlet4' and 't-inlet3' showed highest temperature rise because the fluid penetration and density is low, resulting only diminished amount of heat can be transferred. "t-inlet2' also show similar trend. The temperature of different radial distance reach temperature of 450K, and this occur because no significant heat transfer occur hence the tubes temperature are not cool down.

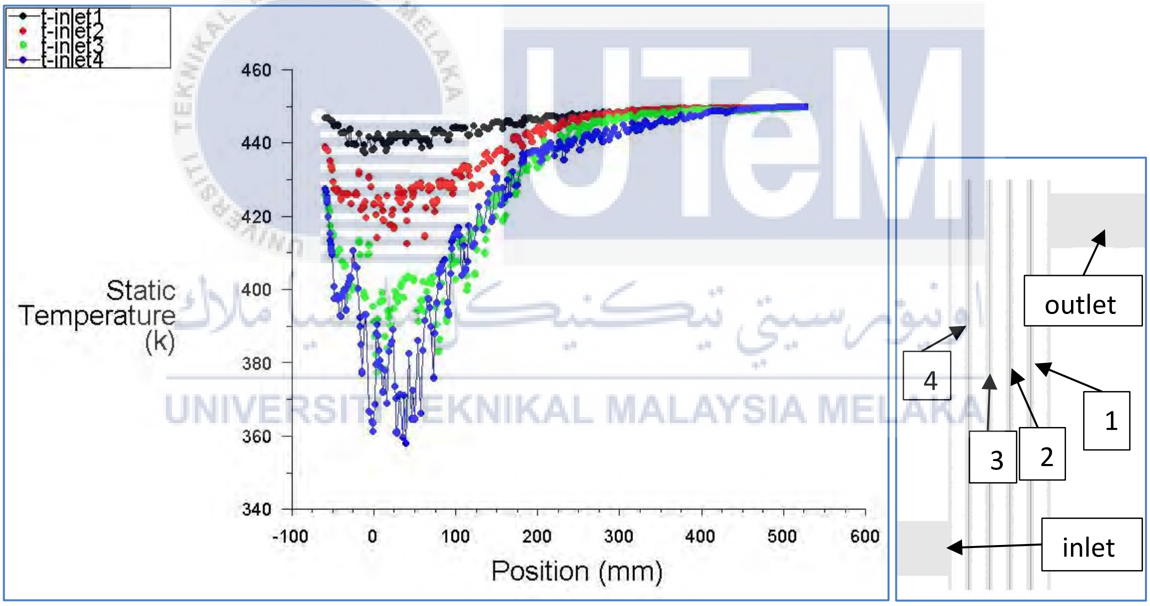

(a) **(b)**

Figure 4.14 (a) Variation of CO_2 temperature with dimensionless axial distance; (b) radial distance: (1) $x/D_s = 0.2$, (2) $x/D_s = 0.4$, (3) $x/D_s = 0.6$, (4) $x/D_s = 0.8$

4.6 Analysis and Discussion

Basically, Ammonia, Isobutane (R600a) and Carbon Dioxide have similar fluid flow at the central plane and the flow recirculation at the outlet. However, when considering the inlet plane, different results are observed. Figure 4.15 shows the inlet flow of R600a, NH_3 and CO_2. In these three figures, Carbon Dioxide flow is the weakest in term of penetration and flow concentration. This is because it is gas hence, it is weaker in transferring heat away. Next is Ammonia (NH_3) and Isobutane (R600a). These two fluids have similar fluid flow behaviour. The only thing that distinguish the two fluids is that R600a have better penetration than Ammonia and it also contains less flow recirculation compared to Ammonia.

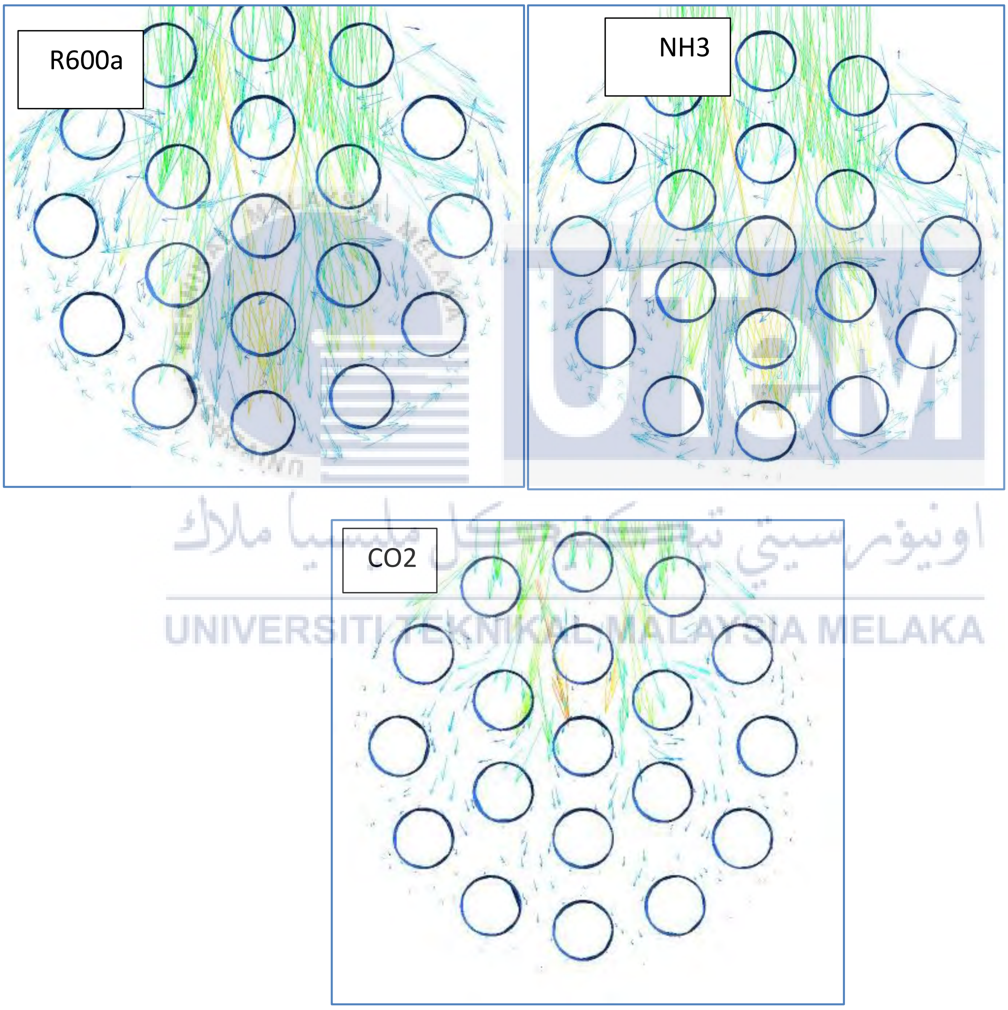

Figure 4.15 Inlet plane flow comparison between R600a, NH3 and CO2

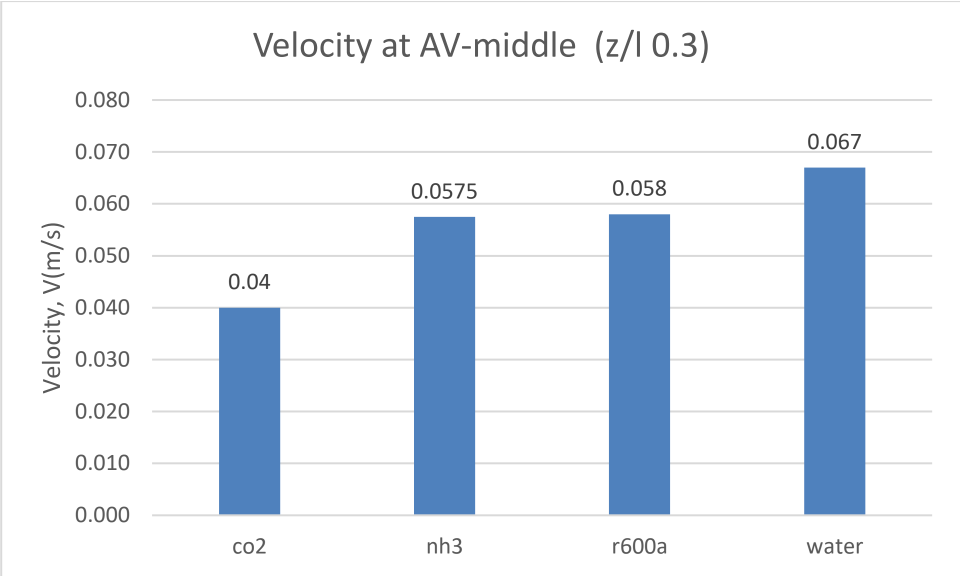

Figure 4.16 Velocity comparison at position z/L=0.3

For velocity distribution, Ammonia, Isobutane and Carbon Dioxide have similar flow pattern. However, they all have different axial velocity. From Figure 4.17, Carbon Dioxide have velocity of 0.04 m/s, Ammonia have velocity of 0.0575 m/s, Isobutane have velocity of 0.058 m/s and water have velocity of 0.067 m/s. The water velocity is obtained from journal by Pal (2016). Isobutane have the highest velocity compared to other fluid because Isobutane have high viscosity. Although Ammonia have similar viscosity with Isobutane, however Ammonia's density is twice of that of the Isobutane, resulting to slower velocity as it requires more energy or pressure difference to flow. However, when comparing water and Isobutane, water have higher velocity than Isobutane. This is because, water has viscosity higher than Isobutane.

Next is the temperature contour from the central, it is obvious that from Figure 4.12(c) that Carbon Dioxide is the weakest heat conductor as there is no significance temperature drop observed. Between Ammonia and Isobutane, Isobutane is a better cooling fluid. Figure 4.16 shows the temperature contour of R600a and NH_3. From the figure, it is observed that the R600a have a better flow penetration as the cooling region reach up to axial distance z/L= 0.8 while Ammonia can only reach up to axial distance z/L = 0.6.

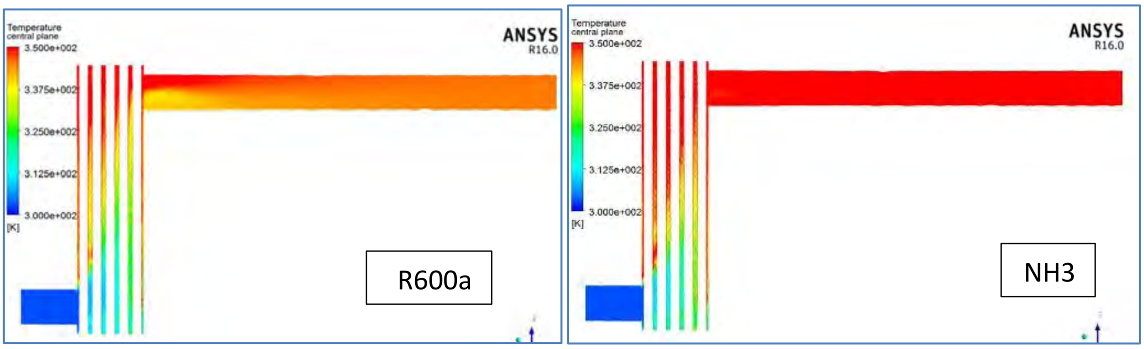

Figure 4.17 Comparison R600a and NH_3 temperature contour at central plane.

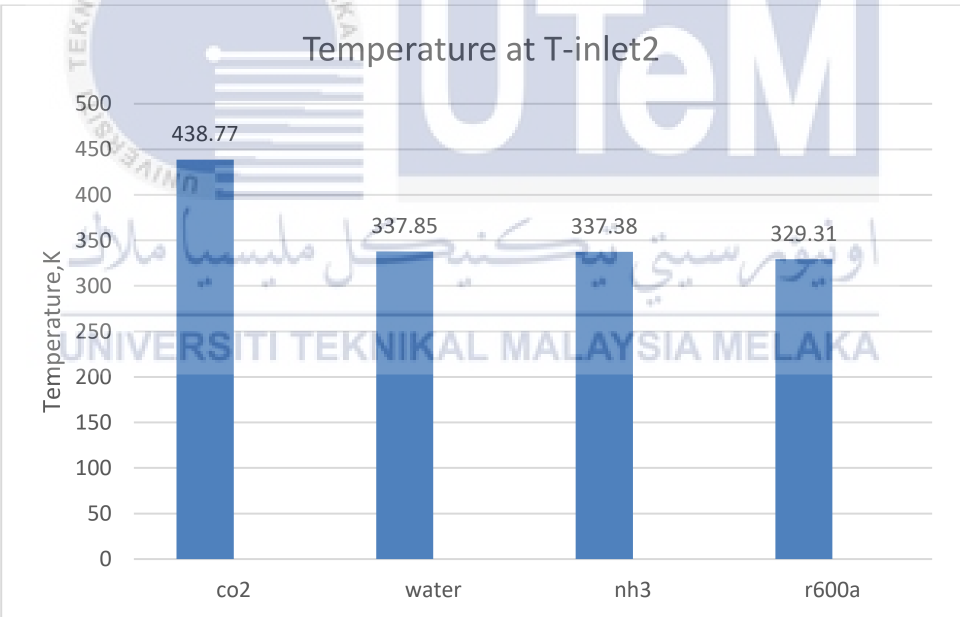

Figure 4.18 Temperature comparison at position x/D_s= 0.2

Lastly is temperature distribution. As Carbon Dioxide have low density and viscosity, hence, it does not have strong fluid penetration resulting to its poor ability in transferring heat. As for the Ammonia and Isobutane, both have similar temperature distribution but comparatively, Isobutane have lower highest temperature which is 380 K compared to

Ammonia with temperature of 390 K. From Figure 4.18, it shows the comparison of temperature at position $x/D_s = 0.4$ of Carbon Dioxide, Water, Ammonia and Isobutane. The position $x/D_s = 0.4$ was chosen because this line is at the centre of the shell and this is the location where the maximum point of the fully developed flow occur. With the maximum velocity, the fluid will penetrate the best hence the heat exchange process will be better too. Among the four fluids, Carbon Dioxide have the highest temperature which is 438.77 K, followed by Water, 337.85 K; Ammonia, 337.38 K and the lowest of all is Isobutane 329.31 K.

CHAPTER 5

CONCLUSION

In conclusion, a functional CFD model of Shell and Tube Heat Exchanger (SNTHE) was created using ANSYS FLUENT version 16. The first objective of this paper is achieved with error of 7 % for the temperature field and 4% for the velocity field. However, derived parameters, such as Reynolds number and heat transfer rate ,have big error. This may be due to incorrect interpretation of formula. The second objective is to compare the temperature distribution of three different coolant in SNTHE. Three coolants; Ammonia, Isobutane and Carbon Dioxide is compared with reference fluid of water in terms of temperature. From Figure 4.18, at $x/D_s = 0.2$, Carbon Dioxide have the highest temperature and Isobutane have the lowest temperature. Higher temperature indicates that it has low capacity to perform heat transfer activity as the heat transfer rate is low. Hence, Isobutane is the best in terms of heat transfer capacity. Third objective is to compare the flow condition of three different coolant in SNTHE. Figure 4.16 showed the velocity at $z/l = 0.3$ and this figure showed that water have the highest velocity followed by Isobutane, Ammonia and Carbon Dioxide. High velocity or high axial velocity represent high capabilities in penetrating inn between the tubes. Isobutane have the best penetration speed compared to the other fluid hence it can carry out heat transfer process better. In conclusion, Isobutane has the potential to be the substitute and alternative for water for cooling process.

In this project, there were several limitations faced. First is the license issues. As a student, only student version ANSYS are accessible and this has limited the simulation to 500000 mesh size only. This is very inconvenient for 3D simulation as it requires high mesh size to obtain more accurate answer. Next is the geometry used in this project. As the objectives is focusing on the flow condition, the presence of baffle in the SNTHE was ignored to simplified the computational domain and focus on flow only. However, ones need to study other area of flow condition such as heat flux, Prandlt number or log mean temperature difference, it is better to use a baffled SNTHE as it can replicate more actual and realistic flow condition. So, in future, to understand better the SNTHE, it is better to use a commercial license and study baffle SNTHE with high mesh size simulation to understand better any performances or flow regarding SNTHE.

REFERENCE

A.Keith Escoe , 1986. Mechanical Design of process System, Gulf Publishign Company

Anas El Maakoul, Azzedine Laknizi, Said Saadeddine, Mustapha El Metoui, Abdelkabir Zaite , Mohamed Meziane, Abdelatif Ben Abdellah , 2016. Numerical comparison of shell-side performance for shell and tube heat exchangers with trefoil-hole, helical and segmental baffles, *Applied Thermal Engineering* Vol. 109, 175–185

Brogan, R.J. ,1985. Heat Transfer and Pressure Drop During Condensation Inside a Horizintal Tube, *HTPS Research Symposium*, pp 637-651

Claudio Zilio, Simone Mancin, 2015. Shell and Tube carbon dioxide gas coolers – Experimental result and modelling, *International Journal of Refreigeration,* 56, 224-234

Eshita Pal, Inder Kumar, Jyeshtharaj B.Joshi , Maheshwari, N.K., 2016. CFD simulations of shell-side flow in a shell-and-tube type heat exchanger with and without baffles, *Chemical Engineering Science*,143, 314–340

Junwei, Huang, Hua, Wang, Huitao, Wang, Zhong, Ge, 2011. Theroritical Analysis of Isobutane as Refrigerant of Air Source Heat Pump, *Third International on Measuring Technology and Mechatronic Automation,* 999-1003

Lachi, M., Wakil, N.el, and Padet, J., 1997. The time constant of double pipe and one pass shell and tube heat exchanger in the case of the varying fluid flow rates. *Int. J. Heat Mass Transfer*. Vol 40. 2067-2079

Madhuri Tayde, Jeevan Wankhade, Shylesa Chanapattana, 2014. Heat Transfer Analysis of a Helically Coiled Heat Exchanger. *Int. J. Innovative Research and Development*, Vol 3, Issue 13, 265-268

Master, B.I., Chunangad, K.S., Boxma, A.J., Kral, D., Stehlík, P., 2006. Most frequently used heat exchangers from pioneering research to worldwide applications, *Heat Transfer Eng*. Vol 27, 4–11

Muhammad Mahmood Aslam Bhutta, Nasir Hayat, Muhammad Hassan Bashir, Ahmer Rais Khan, Kanwar Naveed Admad, Sarfaraz Khan, 2012. CFD applications in various heat exchanger design: A review, *Applied Thermal Engineering*, 32, 1-12

Pekdemir, T., Davies, T.W., Haseler, L.E., Diaper, A.D., 1993. Flow distribution on the shell side of a cylindrical shell and tube heat exchanger, *Int J. Heat and Fluid Flow*, 14, 76-85

Wang, Q., Chen, Q., Chen, Q., Zeng, M., 2010. Review of improvements on shell-and tube heat exchangers with helical baffles, *Heat Transfer Eng*. Vol 31, 836–853.

Yanfeng Zhang, Chen Jiang, Zonglin Yang, Yiyuan Zhang, Bofeng Bai, 2016. Numerical study on heat transfer enhancement in capsule-type plate heat exchangers, *Applied Thermal Engineering*, 108,1237-1242

Yongqing Wang, Xin Gu, Zunlong Jin, Ke Wang, 2015. Characteristics of heat transfer for tube banks in crossflow and its relation with that in shell-and-tube heat exchangers. *International Journal of Heat Transfer*, 93, 584-594

Yunus A.Cengel, Afshin J.Ghajar, 2015. Heat and Mass Transfer: Fundamentals and Application, Fifth edition in SI Units. Mc Graw Hill

Yunus A.Cengel, John M.Cimbala, 2010. Fluid Mechanics: Fundamentals and Applications, Second Edition in SI units. Mc Graw Hill

Zahid H. Ayub, Ahmad Abbas, Adnan H.Ayub, Tariq S. Khan, Javed A.Chatta, 2017. Shell side direct expansion evaporation of ammonia on a plain tube bundle with exit superheat effect, *International Journal of Refrigeration,* 76, 126-135

APPENDIX A: Gantt Chart

Gantt Chart Psm 1

No	Task	Weeks														
		1	2	3	4	5	6	7	8	9	10	11	12	13	14	15
1	Briefing															
2	Introduction (Intro, Objective, Scope)															
3	Literature Review Writing															
4	Progress Report															
5	Methodology															
6	Preprocessing															
7	Final Draft Full Report															

Gantt Chart Psm 2

No	Task	Weeks														
		1	2	3	4	5	6	7	8	9	10	11	12	13	14	15
1	Project Progress Report Updating (Chap 1, 2 ,3)															
2	Validation															
3	Data Processing															
4	Model Analysis															
5	Project Result And Discussion Report Writing (Chap 4)															
6	Project Conclusion Report Writing (Chap 5)															
7	Final Draft Full Report															
8	Seminar And Presentation															
9	Hard Bound															Week 20